Published online 12 May 2022

Critical Reviews and Perspectives

The metaphorical swiss army knife: The multitude and diverse roles of HEAT domains in eukaryotic translation initiation

Daniel Friedrich [1,2,3,*], **Assen Marintchev** [4] **and Haribabu Arthanari** [2,3,*]

[1]Department of Molecular and Cellular Biology, Harvard University, Cambridge, MA, USA, [2]Department of Cancer Biology, Dana-Farber Cancer Institute, Boston, MA, USA, [3]Department of Biological Chemistry and Molecular Pharmacology, Harvard Medical School, Boston, MA, USA and [4]Department of Physiology & Biophysics, Boston University School of Medicine, Boston, MA, USA
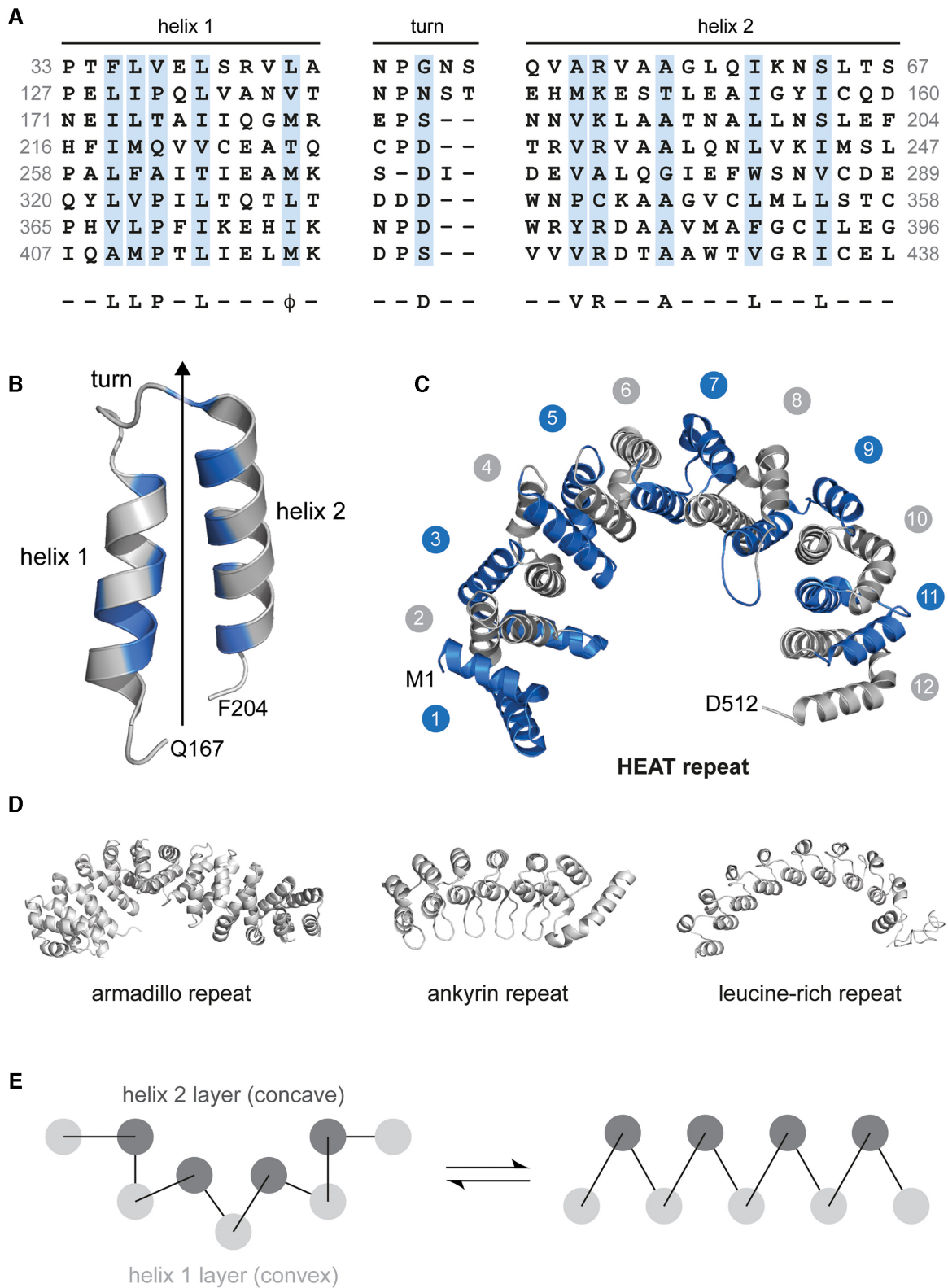
ABSTRACT

Biomolecular associations forged by specific interaction among structural scaffolds are fundamental to the control and regulation of cell processes. One such structural architecture, characterized by HEAT repeats, is involved in a multitude of cellular processes, including intracellular transport, signaling, and protein synthesis. Here, we review the multitude and versatility of HEAT domains in the regulation of mRNA translation initiation. Structural and cellular biology approaches, as well as several biophysical studies, have revealed that a number of HEAT domain-mediated interactions with a host of protein factors and RNAs coordinate translation initiation. We describe the basic structural architecture of HEAT domains and briefly introduce examples of the cellular processes they dictate, including nuclear transport by importin and RNA degradation. We then focus on proteins in the translation initiation system featuring HEAT domains, specifically the HEAT domains of eIF4G, DAP5, eIF5, and eIF2Bε. Comparative analysis of their remarkably versatile interactions, including protein–protein and protein–RNA recognition, reveal the functional importance of flexible regions within these HEAT domains. Here we outline how HEAT domains orchestrate fundamental aspects of translation initiation and highlight open mechanistic questions in the area.

INTRODUCTION

The characteristic architecture of the HEAT domains and the built-in flexibility

In 1995, Andrade and Bork used systematic sequence analyses to identify a specific, repeating motif found in multidomain proteins (1). This motif was detected in four distinct proteins, leading to a designation derived from those protein names, the 'HEAT' repeat: **h**untingtin, eukaryotic translation **e**longation factor 3 (eEF3), the regulatory **A** subunit of protein phosphatase 2A (PP2A), and mechanistic **t**arget of rapamycin (mTOR). The number of these repeating motifs in individual HEAT domains can vary enormously from 3 to 50 and each motif is comprised of approximately 50 residues (2). The conservation of amino acid composition amongst HEAT domains tends to be relatively low as evidenced by a weak consensus sequence (Figure 1A) (3); however, structural conservation is high with the fundamental HEAT motif formed by two anti-parallel, amphiphilic α-helices connected by one turn, arranged about a common axis (Figure 1B) (2). The turn features a conserved aspartate residue that is often found to interact with an arginine side chain in the second helix via a salt bridge. Consensus sequence residues in the two α-helices typically face each other. These basic helix-turn-helix motifs are further connected by linking inter-motif loops. The overall arrangement can result in a curved architecture (Figure 1C), placing HEAT domains in the alpha solenoid protein family (also known as alpha horseshoes), which also includes armadillo, ankyrin and leucine-rich repeats (4) (Figure 1D). This protein family has been found to be involved in many intracellular signaling and transport processes. Examples for leucine-rich repeat-containing proteins are the toll-like re-

---

*To whom correspondence should be addressed. Email: hari_arthanari@hms.harvard.edu
Correspondence may also be addressed to Daniel Friedrich. Email: daniel_friedrich@dfci.harvard.edu

A

	helix 1		turn		helix 2	
33	P T F L V E L S R V L A		N P G N S		Q V A R V A A G L Q I K N S L T S	67
127	P E L I P Q L V A N V T		N P N S T		E H M K E S T L E A I G Y I C Q D	160
171	N E I L T A I I Q G M R		E P S - -		N N V K L A A T N A L L N S L E F	204
216	H F I M Q V V C E A T Q		C P D - -		T R V R V A A L Q N L V K I M S L	247
258	P A L F A I T I E A M K		S - D I -		D E V A L Q G I E F W S N V C D E	289
320	Q Y L V P I L T Q T L T		D D D - -		W N P C K A A G V C L M L L S T C	358
365	P H V L P F I K E H I K		N P D - -		W R Y R D A A V M A F G C I L E G	396
407	I Q A M P T L I E L M K		D P S - -		V V V R D T A A W T V G R I C E L	438

- - L L P - L - - - φ - 　 - - D - - 　 - - V R - - A - - - L - - L - - -

B

C

HEAT repeat

D

armadillo repeat　　　　ankyrin repeat　　　　leucine-rich repeat

E

helix 2 layer (concave)

helix 1 layer (convex)

Figure 1. HEAT domains have a characteristic structure. (**A**) The alignment of HEAT repeat sequences of mouse importin-β highlights a consensus sequence ---LLP-L---φ-....--D--...--VR--A---L--L--- (φ being a hydrophobic residue). (**B**) The characteristic fold of HEAT domains consists of a helix-turn-helix motif arranged about a common axis (PDB code 1gcj); consensus sequence residues are colored in blue according to the alignment shown in (A). (**C**) Twelve repeats (colored in alternating blue and grey) of the yeast importin-β HEAT domain feature an alpha solenoid arrangement (PDB code 3nd2). (**D**) Other members of the alpha solenoid family include armadillo (as example the armadillo repeat region of murine β-catenin, PDB code 3bct), ankyrin (as example the ankyrin domain of the Notch receptor, PDB code 1ot3) and leucine-rich repeats (as example the leucine-rich repeat variant, PDB code 1lrv). (**E**) HEAT domains exhibit high elasticity, facilitating the formation of multiple global structures.

ceptor, the ribonuclease inhibitor, and the tropomyosin regulator tropomodulin; in these proteins, leucine-rich repeats mediate protein–protein interactions with binding partners (5–7). Armadillo repeats are found in various proteins as well, e.g. in β-catenin and α-importin; prominent examples of proteins with ankyrin repeats are Notch and NFκB1 (8–13).

HEAT domains are found in a large variety of proteins, often enabling distinct protein–protein interactions and one of the ways this can be achieved is by structural plasticity, adopting multiple tertiary conformations (1,14–16). The inherent flexibility in the HEAT domain has been experimentally demonstrated using fluorescence spectroscopy and small angle X-ray scattering (17,18). Molecular dynamics simulations further suggested that HEAT domains are highly elastic upon the external application of force (14,19). It is conceivable that such elastic properties provide the structural flexibility required for binding to various interaction partners *in vivo* (Figure 1E). Even though the fundamental unit, the helix-turn-helix motif (Figure 1B), is structurally highly conserved, HEAT domains are capable of adopting multiple, structurally heterogeneous global architectures (Figure 1E). This diversity is reflected in the plethora of processes in which HEAT domains are involved, ranging from nucleocytoplasmic transport to chromatin remodeling (3,20–22), thus establishing HEAT domains as a fundamental building block deployed by the cell to accomplish a variety of essential processes.

HEAT domains orchestrate vital cellular processes in eukaryotes

HEAT repeats form versatile higher order architecture that can mediate both protein–protein and protein–nucleic acid interactions (23–25). In this section we will highlight a few illustrative examples of HEAT domain-containing proteins that regulate key cellular functions, including mediators of nuclear transport, chromatin remodeling, protein dephosphorylation and RNA degradation. The archetypal examples are the four eponymous proteins: huntingtin, eEF3, PP2A and mTOR. Mutations in huntingtin that introduce a poly-glutamine sequence lead to aggregation, resulting in neuron degeneration (26,27). eEF3 is an essential factor for translation elongation found in fungi (28–30). In eukaryotic cells, the structural subunit of the ubiquitously expressed phosphatase PP2A, a classic example of an alpha solenoid structure consisting of HEAT repeats (1,31–32), contributes significantly to cellular phosphatase activity, dephosphorylating important signaling factors such as RAF, MEK or AKT (33–35). Lastly, the function of mTOR involves HEAT domains as well (36–38). mTOR forms two complexes (mTORC1 and mTORC2), both of which serve as central hubs for multiple signaling networks within the cell (39,40), involving them in the sensing of nutrients, energy and redox potentials and the regulating of the actin cytoskeleton, protein synthesis, and survival and metabolism (41,42).

The diversity of roles and pathways for these four proteins is a testament to the versatility of HEAT domains. In addition to these four classic examples, there are other notable cases that highlight how these repeats critically

contribute to cellular function. The ataxia-telangiectasia mutated serine/threonine kinase (ATM) and the DNA-dependent protein kinase catalytic subunit (DNA-PKcs) are both chromosome-associated factors that harbor large, flexible HEAT scaffolds (3,43). Nuclear transport mediated by importin is another well-studied case of a fundamental cellular process involving HEAT repeats (44,45). Belonging to the karyopherin family, importin recognizes proteins as cargo through their nuclear localization sequences (NLS) and directs them into the nucleus through the nuclear pore complex (46–48). Importin consists of two subunits, α and β, and it is the β-subunit that has a characteristic HEAT domain, containing nineteen repeats of the basic helix-turn-helix motif (44,49). Finally, HEAT domains are also directly involved in mediating protein–nucleic acid interactions. The Ro protein and its HEAT repeat-mediated binding to RNA, for example, have been studied extensively over the past few decades (25,50–54). Structural studies have shown that Ro consists of two domains, one adopting a Rossmann fold, while the other is a HEAT domain arranged in a toroid-like shape.

These examples outline the remarkable versatility of HEAT domains in mediating protein–protein and protein–nucleic acid interactions. In the following sections, we will focus exclusively on HEAT domains in proteins essential for eukaryotic translation initiation.

DISCUSSION

The multifaceted role of HEAT domains in eukaryotic translation initiation

HEAT domains feature prominently among proteins involved in eukaryotic translation. To our knowledge, more than ten different proteins which are translation initiation factors or regulators of protein synthesis, ranging in size from about 50 kDa (basic leucine zipper and W2 domain-containing protein (BZW)) to 300 kDa (eIF2α kinase activator GCN1), harbor HEAT domains. Some of them are schematically shown in Figure 2. Notably, the HEAT domains in most of these proteins share a common ancestor and can be classified into three groups, based on sequence homology and structure (55–57).

The first group, defined by the so-called middle domain of eukaryotic translation initiation factor 4G (MIF4G), contains five to seven repeats of the basic helix-turn-helix motif (Figure 2) (55,58). As the most N-terminally located HEAT domain in both isoforms of eukaryotic initiation factor 4G (eIF4G, the isoforms are commonly termed eIF4GI and eIF4GII; the latter, however, is also abbreviated as eIF4G3 in online sequence databases), MIF4G is also often referred to as HEAT1 in the literature (58–61). In addition to being located in eIF4G, the MIF4G/HEAT1 domain is found in a number of other translation factors and regulators, including the eIF4G homolog death-associated protein 5 (DAP5; also known as p97, NAT1 or, in online sequence databases, eIF4G2), nuclear cap-binding protein subunit 1 (NCBP1), the CBP80/20-dependent translation initiation factor (CTIF) (62), the SLBP-interacting protein 1 (SLIP1), required for translation initiation of histone mRNAs that have a 3′ stem-loop but no poly-A tail (63), the *Drosophila* protein Mextli, which appears to function as
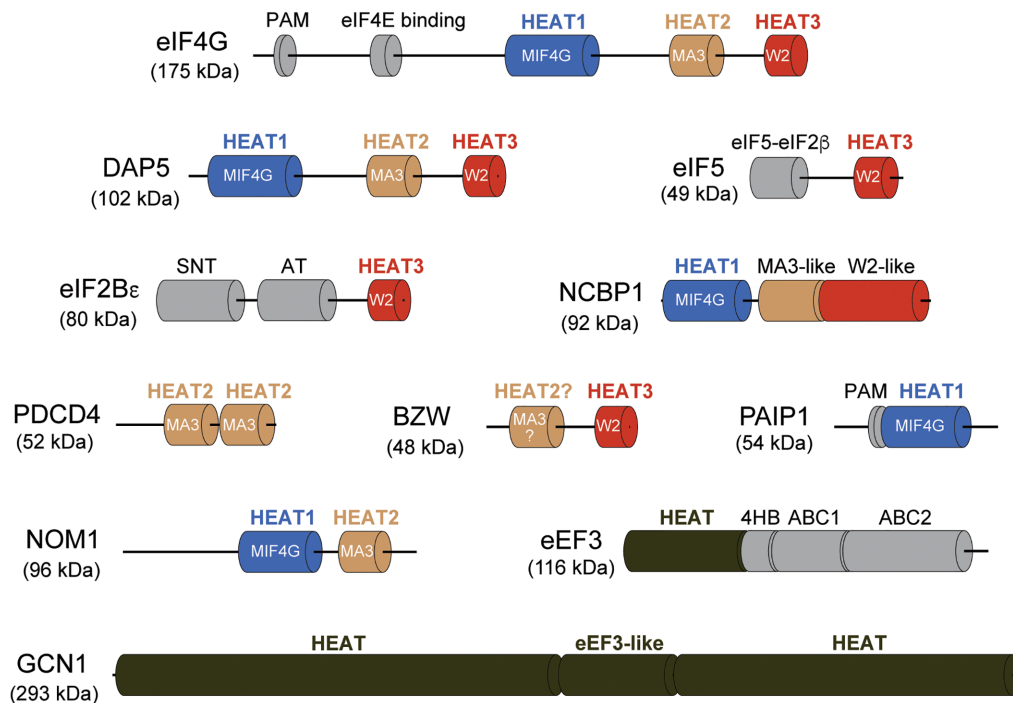
Figure 2. HEAT domain-containing proteins involved in protein synthesis. In most of the proteins discussed in the main text that contribute to translation control, HEAT domains can be grouped in three classes (based on their sequences): middle domain of translation initiation factor 4G (MIF4G, also termed HEAT1 (blue)), MA3 (also termed HEAT2 (brown)) and W2 (also termed HEAT3 (red)) domains. Non-HEAT domains and binding motifs are shown in light grey and HEAT domains in colors and black. eIF4G = eukaryotic initiation factor 4G (UniProtKB Q04637); DAP5 = death-associated protein 5 (UniProtKB P78344); eIF5 = eukaryotic initiation factor 5 (UniProtKB P55010); eIF2Bε = eukaryotic initiation factor 2Bε (UniProtKB Q13144); NCBP1 = nuclear cap-binding protein subunit 1 (UniProtKB Q09161); PDCD4 = programmed cell death protein 4 (UniProtKB Q53EL6); BZW = basic leucine zipper and W2 domain-containing protein (UniProtKB Q9Y6E2); PAIP1 = polyadenylate-binding protein interacting protein 1 (UniProtKB Q9H074); NOM1 = nucleolar MIF4G domain-containing protein 1 (UniProtKB Q5C9Z4); eEF3 = eukaryotic translation elongation factor 3 (UniProtKB P16521); GCN1 = eIF2α kinase activator general control nonderepressible 1 (UniProtKB Q92616); PAM = polyadenylate-binding protein interaction motif; SNT = sugar-nucleotidyl transferase-like; AT = acyl transferase-like; 4HB = four helical bundle domain; ABC = ATP-binding domain of ABC transporters. All proteins illustrated here are derived from *H. sapiens*, except eEF3 which is from *S. cerevisiae*.

an eIF4E-binding protein (64), the Up-frameshift suppressor 2 (UPF2), which has three MIF4G domains, involved in nonsense-mediated decay (NMD) of mRNAs containing premature stop codons by associating with the nuclear exon junction complex (EJC) (65), the polyadenylate-binding protein-interacting protein 1 (PAIP1), and the nucleolar MIF4G domain-containing protein 1 (NOM1) (Figure 2). NOM1 is involved in ribosome biogenesis and interacts with eIF4A3, a DEAD box ATPase involved in alteration of RNA secondary structure (66,67).

The second group is represented by the MA3 domain (Figure 2) (55,56), also known as the HEAT2 domain (61,68–71), and is typically formed by three to four HEAT repeats. This class of HEAT domains is also found in eIF4G, DAP5, programmed cell death protein 4 (PDCD4), and NOM1 (Figure 2) (56,58,68,72–78). BZW has also been suggested to feature a MA3/HEAT2 domain (79), but this has not yet been experimentally confirmed.

The third group constitute the W2 domains, termed after two invariant tryptophan residues (Figure 2) (56,68,80). These W2 HEAT domains are found at the C-termini of eIF4G, DAP5, eIF5, eIF2Bε, and BZW (57,68,81–86). In line with the nomenclature for the MIF4G/HEAT1 and MA3/HEAT2 domains and due to its C-terminal location in eIF4G, the W2 domain is also termed HEAT3

(56). MA3-like and W2-like HEAT domains are also found in NCBP1, C-terminal to its MIF4G/HEAT1 domain (79).

In addition to the proteins containing MIF4G/HEAT1, MA3/HEAT2 and W2/HEAT3 domains, characteristic HEAT repeats can also be found in other proteins involved in the regulation of translation. These include the fungal protein eEF3 and GCN1 that features an eEF3-like HEAT domain (Figure 2). There is evidence that GCN1 is composed almost exclusively of HEAT repeats, which extend both N- and C-terminal of its eEF3-like domain as indicated by secondary structure predictions and recent cryo-electron microscopy-derived structural information (87–89). The HEAT domains found in these proteins are distinct, showing no sequence homology to the above three HEAT domain classes. Other HEAT domain-containing proteins, such as the La-related protein 1 (LARP1) and Listerin, are structurally most closely related to importin-β. LARP1 is a regulator of translation of 5′ terminal oligopyrimidine (TOP) mRNAs. Listerin is an E3 ubiquitin-protein ligase component of the ribosome quality control complex (RQC). In addition, there are many other proteins that have helical hairpin repeat domains structurally related to the HEAT domains. For example, six of the 13 subunits of mammalian eIF3 are members of the proteasome, COP9

signalosome, eIF3 (PCI) family of proteins, structurally closely related to the HEAT family (90).

All the proteins described in the section above are involved in mRNA translation. In the critical translation initiation phase, both 5′ 7-methylguanosine (m⁷G) cap-dependent and cap-independent mechanisms are known (91). The latter has been shown to contribute to regulation of cell fate decisions in the context of cancer and cellular differentiation, and plays an important role in viral replication (92).

Initiation of cap-dependent translation

A number of eukaryotic initiation factors have been thoroughly characterized providing a detailed mechanistic understanding of canonical, i.e. cap-dependent translation initiation (93). In this process, the initial step is assembly of the cap binding trimeric complex eIF4F, in which eIF4E recognizes the mRNA 5′cap, and the scaffolding initiation factor eIF4G binds to eIF4E and recruits the RNA helicase eIF4A, an interaction mediated by the MIF4G/HEAT1 and MA3/HEAT2 domains of eIF4G. Initially, eIF4A unwinds secondary structures in the 5′-untranslated mRNA region (5′UTR) of the mRNA in the vicinity of the cap, with the help of eIF4G and eIF4B. Subsequently, eIF4G recruits the 43S pre-initiation complex which scans the 5′UTR with continued unwinding of the mRNA by eIF4A. When the start codon (AUG) in a proper sequence context is identified, the 48S pre-initiation complex is formed and a subset of the eIFs are released upon GTP hydrolysis by eIF2. eIF2 is replaced at the Met-tRNA$_i^{Met}$ by eIF5B, another GTPase, which promotes engagement with the 60S ribosomal subunit to form the 80S ribosome, competent to proceed with the elongation step. It is well established that assembly of eIF4F is inhibited by sequestering eIF4E under cellular stress conditions, thereby suppressing cap-dependent and presumably promoting cap-independent translation initiation mechanisms (93).

Of the various HEAT domain-featuring proteins involved in protein synthesis, eIF4G and its homolog DAP5, eIF5, and eIF2Bε play particularly crucial roles in translation initiation. Since high-resolution structures of the HEAT domains of these proteins have been published, we analyzed their structural properties to highlight the multiple functions of HEAT domains in translation initiation.

Functions of HEAT domain-containing translation initiation factors

The translation initiation factors eIF4G, DAP5, eIF5, and eIF2Bε have specific and distinct functions in the first phase of protein synthesis. As introduced in the previous section, eIF4G plays an essential role in recruiting the pre-initiation complex to mRNA in cap-dependent translation by binding eIF4E (Figure 3A), which recognizes the m⁷G 5′cap, eIF4A, ensuring mRNA unwinding, and polyadenylate-binding protein (PABP), which induces mRNA circularization (94–98). As the major scaffolding initiation factor, eIF4G also promotes binding of the 40S ribosomal subunit to the mRNA by interacting with eIF3 and the 40S subunit directly (59,99–102). eIF4G, which has three HEAT

domains in total (Figure 2), exists as two isoforms, eIF4GI and eIF4GII (also known as eIF4G3), with the former being more abundant (93,103–104). The isoforms are encoded by separate genes, and although their functions are similar, there is evidence that they may exhibit some selectivity bias towards different mRNAs (93). Playing a distinct role to eIF4G, its homolog DAP5 has the same HEAT domain organization and homology with the C-terminal two thirds of eIF4G (Figure 2). However, as DAP5 lacks the ability to bind PABP and eIF4E, it promotes non-canonical translation initiation mechanisms by recruiting the ribosome, including via internal ribosome entry sites (IRESs) in 5′UTRs of mRNAs (Figure 3A) (105–109). It has been suggested that DAP5 can also promote an alternative cap-dependent mechanism by utilizing eIF3d (110).

eIF5 is another HEAT domain-containing factor directly involved in translation initiation. Similar to eIF4G, DAP5, and eIF2Bε, it has a C-terminal W2/HEAT3 domain (Figure 2) (83,84). eIF5 joins the 43S pre-initiation complex through specific binding to eIF2-GTP and eIF3c (Figure 3A), as well as eIF1 and eIF1A (83,93,111–113). eIF5 acts as the GTPase-activating protein of eIF2, which brings the Met-tRNA$_i^{Met}$ to the pre-initiation complex (114,115). Upon start codon recognition, GTP hydrolysis, and phosphate release, eIF5 dissociates together with eIF2-GDP from the pre-initiation complex (116–120). eIF2-GDP, which is released after every round of translation initiation, is then recycled to form a new eIF2-GTP:Met-tRNA$_i^{Met}$ ternary complex (Figure 3A). This recycling function is performed by the guanine nucleotide exchange factor eIF2B, which substitutes GTP for GDP on eIF2 and promotes Met-tRNA$_i^{Met}$ binding to the eIF2-GTP complex (121–123). Structurally, eIF2B consists of two copies each of five subunits, α, β, γ, δ, and ε, the last of which features a W2/HEAT3 domain at its C-terminus that actually functions as the catalytic domain of the protein, again highlighting the functionality of HEAT domains (Figure 2) (124,125).

The interaction network nucleated by HEAT domains in translation initiation

The wide diversity of interactions mediated by the HEAT domains of eIF4G, DAP5, eIF5 and eIF2Bε is remarkable (Figure 3B). The MIF4G/HEAT1 domains of eIF4G and DAP5 are involved in binding to eIF4A and eIF3 (Figure 3B) (58,69,73,83,102,126–128); some contribution to eIF3 interaction is mediated by the intrinsically disordered region (IDR) in eIF4G, located C-terminally of the MIF4G/HEAT1 domain (129–131). In the case of eIF4G, the MIF4G/HEAT1 domain has also been shown to bind to RNA as well as protein, as demonstrated by studies on the encephalomyocarditis virus IRES (59). The DAP5 MIF4G/HEAT1 domain is capable of binding RNA as well (109,132). Whereas the MA3/HEAT2 domain of eIF4G serves as a second interaction site for eIF4A binding, interaction partners for the MA3/HEAT2 domain of DAP5 have not yet been identified (Figure 3B) (73,76,128,133).

The W2/HEAT3 domains of both eIF4G and DAP5 recruit mitogen-activated protein (MAP) kinase-interacting serine/threonine-protein kinase 1/2 (MNK1/2) via a di-
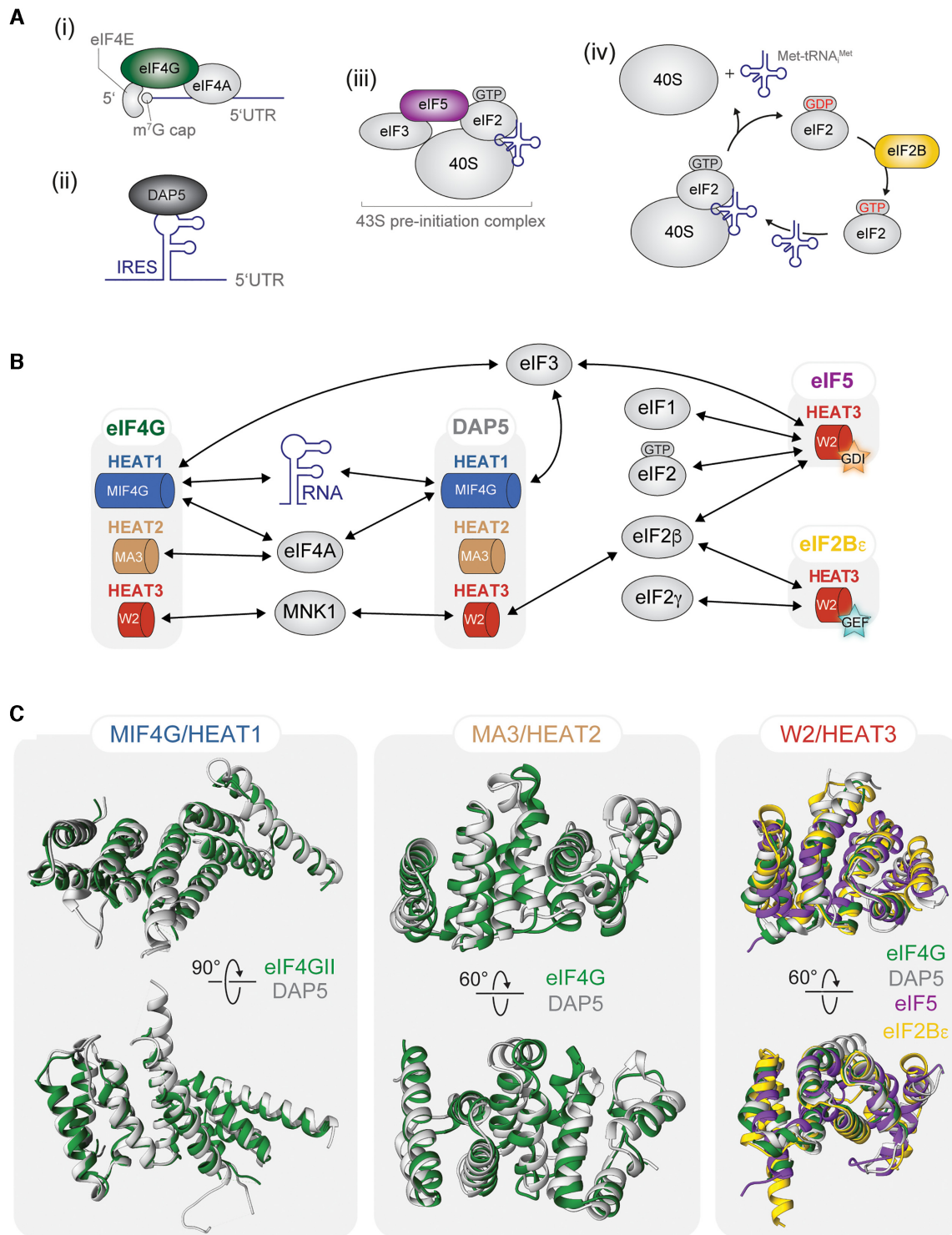
Figure 3. eIF4G, DAP5, eIF5 and eIF2Bε mediate their functionality through structurally highly similar HEAT domains. (**A**) (i) In canonical cap-dependent translation initiation, eIF4G (green) binds to cap-binding eIF4E and the RNA helicase eIF4A. (ii) DAP5 (dark grey) has been shown to promote cap-independent translation initiation events, such as binding of internal ribosome entry sites (IRESs) in 5′ untranslated regions (5′UTRs) in mRNAs with subsequent recruitment of the ribosome. (iii) eIF5 (purple) binds to eIF3 and eIF2-GTP, associated with the Met-tRNA$_i$^Met, to form the 43S pre-initiation complex. (iv) Formation of the 43S translation pre-initiation complex depends on regeneration of the eIF2-GTP:Met-tRNA$_i$^Met ternary complex. Upon GTP hydrolysis, eIF2 dissociates and the guanine nucleotide exchange factor eIF2B (yellow) promotes GDP–GTP exchange on eIF2 and Met-tRNA$_i$^Met binding to form a new complex. (**B**) HEAT domain-mediated interactions of eIF4G, DAP5, eIF5 and eIF2Bε with RNA, other translation initiation factors, and MNK1. GDI = GDP dissociation inhibitor; GEF = guanine nucleotide exchange factor. (**C**) Overlays of MIF4G/HEAT1 (*left panel*), MA3/HEAT2 (*middle panel*) and W2/HEAT3 (*right panel*) domains of DAP5 (grey), eIF4GII/eIF4G (green), the ε-subunit of eIF2B (yellow), and eIF5 (purple). PDB codes: eIF4GII MIF4G/HEAT1 1hu3; DAP5 MIF4G/HEAT1 4iul; eIF4G MA3/HEAT2 1ug3; DAP5 MA3/HEAT2 3l6a; eIF4G W2/HEAT3 1ug3; DAP5 W2/HEAT3 3d3m; eIF5 W2/HEAT3 2iu1; eIF2Bε W2/HEAT3 3jui.

rect interaction between the N-terminal disordered region of MNK1/2 and the W2/HEAT3 domain. MNK1/2 interacts with MAP kinase (MAPK) 1, thus establishing a link between the regulation of translation initiation and the MAPK/extracellular signal-regulated kinase (ERK) pathway (134,135). MNK1/2 phosphorylates the cap-binding protein eIF4E at serine 209, thereby promoting canonical translation initiation of select mRNAs (134,136–137). In the case of DAP5, the same W2/HEAT3 domain has also been shown to interact with the N-terminal tail (NTT) of eIF2β, yet another interaction with a disordered region of a protein (133).

The W2/HEAT3 domains of eIF5 and eIF2Bε also bind to the eIF2β−NTT, but form interactions distinct from those of the eIF4G and DAP5 W2/HEAT3 domains (Figure 3B). The eIF2Bε W2/HEAT3 domain interacts with the γ subunit of eIF2 (138–140), while the eIF5 W2/HEAT3 domain mediates binding to eIF1, eIF1A, and eIF3c (83,120,141–144). In contrast, through their MIF4G/HEAT1 domains, eIF4G and DAP5 interact with a different portion of eIF3, which is located on the solvent surface of the 40S ribosomal subunit (Figure 3B) (102,110,145–146). Most notably, the W2/HEAT3 domains of eIF5 and eIF2Bε have additional, stand-alone functionality in translation initiation. In eIF5, the W2/HEAT3 domain contributes to the GDP dissociation inhibitor (GDI) activity by blocking eIF2B access to eIF2–GDP. In eIF2Bε, the guanine nucleotide exchange factor for eIF2, the W2/HEAT3 domain is the catalytic domain mediating nucleotide exchange (Figure 3A and B) (147–150). When eIF2–GDP is released together with eIF5 from the 48S complex, the eIF2Bε W2/HEAT3 domain is partially responsible for displacement of the eIF5 W2/HEAT3 domain from eIF2β–NTT, thus contributing to the GDI dissociating factor activity of eIF2B (147,151–152). This demonstrates how HEAT domains can contribute functionality in different ways within the same eukaryotic translation initiation pathway.

A view at the HEAT domains through a structural lens

Molecular structures of the HEAT domains in eIF4G, DAP5, eIF5 and eIF2Bε have been determined by X-ray crystallography (Figure 3C) (58,68,84,86,127,153–154). Comparison of structures of the DAP5 and eIF4GII MIF4G/HEAT1 domains reveals a high degree of structural similarity between them, with only minor differences as detailed in the following paragraphs. The overall fold resembles the characteristic HEAT repeat-based shape with most of the α-helices overlaying well, even though they share only 43% sequence identity in structure-based sequence alignments (127). The strongest differences are found in orientations for some of the α-helices and, even more pronounced, two loops that are longer in DAP5 than in eIF4GII.

Structural differences between the MA3/HEAT2 domains of DAP5 and eIF4G are even more subtle (68,153). Superposition of the two shows in both cases a remarkably compact structure with well-aligning α-helices (Figure 3C). Loops connecting the α-helices are rather short in both structures, presumably limiting the degree of freedom

to achieve larger structural variations. However, differences in orientation of the α-helices in the first repeat may mediate distinct functionalities through modulating the interaction with eIF4A as the eIF4G MA3/HEAT2 domain contributes to eIF4A binding, which has not been reported for the MA3/HEAT2 domain of DAP5 (see above and Figure 3B).

Comparison of W2/HEAT3 domain structures of eIF4G, DAP5, eIF5 and eIF2Bε highlights similar characteristic α-helical organization, as expected (Figure 3C). Some differences are observed in length and orientation of α-helices in the first and last HEAT repeats of the domains. Since no significant structural differences between the W2/HEAT3 domains of DAP5 and eIF4G are found, both are expected to bind similarly to MNK1/2. In fact, similar binding affinities for both have been indicated by comparative co-immunoprecipitation experiments of endogenous MNK1/2 (134). As, unlike eIF4G, DAP5 lacks the eIF4E-binding site (Figure 2), it is not immediately obvious why DAP5 would recruit MNK1/2. It is conceivable that DAP5 inhibits cap-dependent translation by competing with MNK1/2–eIF4G binding through sequestering MNK1/2 and thereby decreasing eIF4E phosphorylation levels. While most kinases phosphorylate specific residues in defined consensus sequences, no such consensus sequence is known for MNK1/2. Instead, MNK1/2 binds to eIF4G and phosphorylates eIF4E in the eIF4F complex. Thus, MNK1/2 specificity appears to be driven by its site of recruitment. Another reason for MNK1/2–DAP5 interaction would be the possibility of MNK1/2-mediated phosphorylation of DAP5. Only a few of the putative phosphorylation sites in DAP5 have been studied experimentally (155). Alternatively, other proteins that bind to DAP5 are possible targets for MNK1/2-phosphorylation, similar to eIF4G-aided eIF4E phosphorylation by MNK1/2. The functional relevance and the underlying mechanism of DAP5–MNK1/2 binding remain to be explored. The reported binding of DAP5 to eIF2β–NTT is also puzzling. As in the case of eIF4G, if DAP5 interacts with eIF3 and eIF4A at the solvent surface of the 40S ribosomal subunit, it would be positioned far away from eIF2, which is on the opposite, interface surface of the 40S ribosome subunit.

Compared to the differences between eIF4G and DAP5 HEAT domains, more pronounced structural variation is found in the eIF2Bε and eIF5 W2/HEAT3 domains, in particular in the first HEAT repeat (Figure 3C). This is not surprising as eIF2Bε and eIF5 perform very different functions than eIF4G and DAP5, which additionally have MIF4G/HEAT1 and MA3/HEAT2 domains (156). Taken together, comparing the global structures and folds of MIF4G/HEAT1, MA3/HEAT2 and W2/HEAT3 domains provides only limited insight into mechanistic and functional differences and similarities among eIF4G, DAP5, eIF5, and eIF2Bε. For example, it is not directly obvious from this structural analysis how MIF4G/HEAT1 domains recognize RNA structures and interact with them. The role of MNK1/2 binding to the W2/HEAT3 domain of DAP5 remains unresolved and needs to be studied in more detail. To address the question how the HEAT domains interact with RNA and proteins and what factors

dictate specificity, we analyzed electrostatic potentials, hydrophobicity and evolutionary conservation of their surfaces and binding studies below, focusing on specific examples of MIF4G/HEAT1 interactions with eIF4A and RNA, and W2/HEAT3 binding to eIF2β and MNK1/2.

The interactions of eIF4A with both the eIF4G and the DAP5 MIF4G/HEAT1 domains are based on similar binding mechanisms

As discussed in the previous section, the HEAT domain structures of DAP5, eIF4G, eIF2Bε and eIF5 are very similar with minor deviations. This is not surprising as HEAT domains generally share high structural similarities, albeit having low sequence homology (1,4,16). Thus, comparative analyses of MIF4G/HEAT1 and W2/HEAT3 domain interactions might provide mechanistic insight by revealing binding modes. We therefore studied the interaction sites on eIF4G and DAP5 MIF4G/HEAT1 domains that would engage eIF4A and RNA in more detail (Figure 4). To this end, we employed the *S. cerevisiae* complex structure of eIF4G MIF4G/HEAT1 and eIF4A determined by X-ray crystallography (Figure 4A) (126). eIF4A features an N-terminal and a C-terminal domain, both of which interact with eIF4G MIF4G/HEAT1. Here we separate the potential interaction sites into three distinct interfaces on the surface of the eIF4A domains (Sites 1–3) (Figure 4A). The N-terminal domain interacts with MIF4G/HEAT1 through one specific site (Site 1) and the C-terminal domain has two interaction sites (Site 2 and Site 3). Residues participating in the interaction have been identified by mutagenesis earlier (58). A recent cryo-electron microscopy-based structural model indicates that eIF4G MIF4G/HEAT1 and eIF4A interact through these sites in the context of a reconstituted human 48S translation initiation complex (157). At Site 3, eIF4G binds to eIF4A using a short motif that is linked via Loop$_{582–600}$ to the eIF4G MIF4G/HEAT1 domain (Figure 4A). In this short motif, a highly conserved tryptophan residue (579 in *S. cerevisiae* eIF4G) has been shown by mutational studies to play a significant role in the interaction; however, this is not necessarily the case for DAP5 (126,127). Loop$_{582–600}$ is not resolved in the crystal structure, suggesting that it may remain flexible in the complex. Similarly, one can assume that eIF4G/DAP5 residues that interact with eIF4A at Site 3 are also flexible when eIF4G/DAP5 are not bound to eIF4A. The two domains of eIF4A are continuously moving with respect to each other as the helicase unwinds the mRNA. Therefore, structural flexibility of Loop$_{582–600}$ may provide a mechanistic basis for maintaining high affinity binding between eIF4A and eIF4G as the conformation of eIF4A changes. Leveraging the similarity between the MIF4G/HEAT1 domains of yeast eIF4G and human DAP5, we modeled the DAP5 MIF4G/HEAT1 domain into the complex structure, similar to what has been done earlier by Virgili et al. (127). A large number of residues in the eIF4G/eIF4A binding interfaces are well-conserved between eIF4G and DAP5 (127). This model thus enabled us to discuss MIF4G/HEAT1–eIF4A complex formation and strongly suggests that eIF4G and DAP5 have very similar modes of binding eIF4A.

eIF4G and DAP5 MIF4G/HEAT1 domains engage RNA presumably through different binding modes

Beyond MIF4G/HEAT1–eIF4A binding, we also sought to find indications for MIF4G/HEAT1–RNA interaction sites. As discussed above, both eIF4G and DAP5 MIF4G/HEAT1 domains bind to RNA. Since no high-resolution molecular structures for such interaction are available, we investigated how RNA binding sites of eIF4A relate to the ones of eIF4G/DAP5 interaction to eIF4A. A structure of eIF4A bound to RNA has been solved recently, which includes the eIF4A inhibitor Rocaglamide A (RocA) and the non-hydrolyzable ATP analogue AMP-PNP (Figure 4B) (158). The short, ten nucleotide long RNA in this complex binds to eIF4A at the opposite side of the eIF4G/DAP5–eIF4A interaction sites, suggesting that a longer RNA would have to fold back along the eIF4A surface to the eIF4G or DAP5 MIF4G/HEAT1 domains to enable their interaction with RNA (59,109,132,159–160). Since eIF4G and DAP5 orchestrate different mechanisms of translation initiation, we analyzed structural signatures embedded in the surface of their MIF4G/HEAT1 domain. To this end, we compared the binding sites to eIF4A based on the model in Figure 4A, and the ones to the binding to IRESs as suggested by mutational studies (Figure 4C) (58). As revealed by our and earlier models, the sites for eIF4A binding are located in the same areas on eIF4G and DAP5 MIF4G/HEAT1 (127); Site 3 is not resolved in the DAP5 MIF4G/HEAT1 structure. Hence, differences and similarities regarding flexibility and length of Loop$_{582–600}$ and the sequence contributing to Site 3 remain elusive. Tryptophan 579 is conserved in DAP5, indicating a similar contribution of Site 3 to the mode of binding to eIF4A, even though such interaction has not been reported yet (127). Restrictively, we also would like to note that experimental evidence for eIF4A interaction sites in DAP5 MIF4G/HEAT1 is still missing. The proposed residues involved in IRES binding are based on mutational studies of eIF4G (58). These experiments also suggested a specific loop, 13 amino acids in length (residues 819–832 in human eIF4G), to contribute to IRES binding (specifically residues 823–831). However, this loop is not fully resolved in available eIF4G MIF4G/HEAT1 crystal structures. In human eIF4G, residues 823–831 are not resolved, but electron density is missing only for three residues in the yeast crystal structure (residues 686–688 in Loop$_{677–691}$) (Figure 4C). In contrast, sufficient electron density is observed for the complete loop in DAP5 MIF4G/HEAT1 (residues 142–161), where the loop is also seven residues longer than in eIF4G. Therefore, the proposed IRES interaction site is larger in the case of DAP5 compared to eIF4G in Figure 4C. Since the loop adopts different conformations in the eIF4G and DAP5 structures, the respective surface area varies. More recently, mutational studies of eIF4G MIF4G/HEAT1 further suggested the involvement of two specific aromatic residues in IRES binding, phenylalanines 812 and 978 (59). Aromatic amino acid side chains have been shown to play an important role in protein–nucleic acid interactions, specifically through π–π stacking with adenine (161,162). The role of F812 in engaging the IRES agrees well with earlier studies (58).
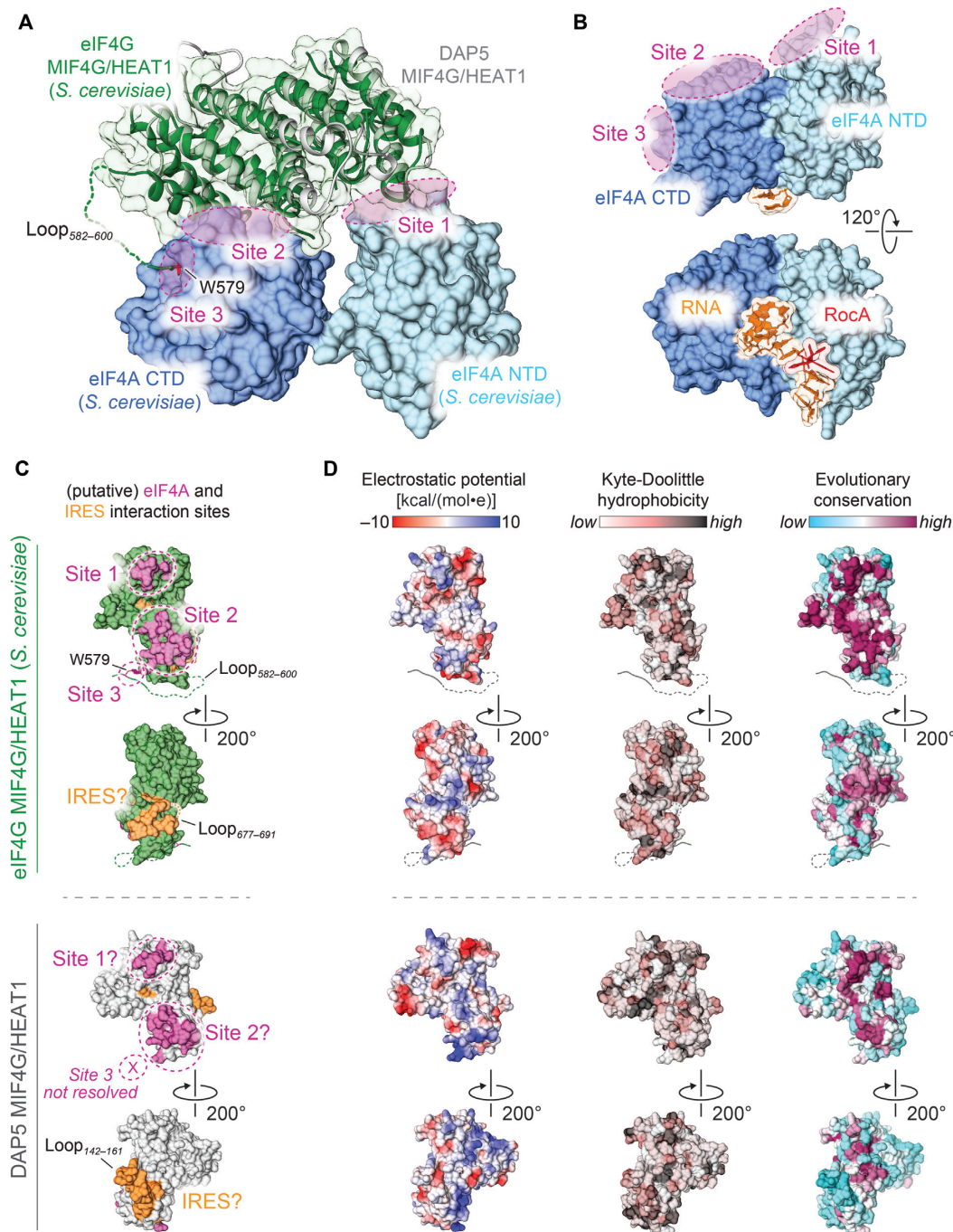
Figure 4. The MIF4G/HEAT1 domains of eIF4G and DAP5 have similar interactions to eIF4A, but putatively different ones to IRESs. (**A**) Crystal structure of the *S. cerevisiae* complex of eIF4G MIF4G/HEAT1 domain (green) and eIF4A (C-terminal domain in dark blue and N-terminal domain in light blue) (PDB code 2vso). The three interaction sites are indicated in magenta; Site 3 contains a highly conserved W579 residue that is further discussed in the main text. As indicated by the dashed ribbon representation, no electron density is available for Loop$_{582–600}$ that links residues participating in Site 3 to the MIF4G/HEAT1 domain. The human DAP5 MIF4G/HEAT1 domain (grey, PDB code 4iul) is modeled into the complex, superimposing the yeast eIF4G MIF4G/HEAT1 domain. (**B**) Crystal structure of human eIF4A in complex with polypurine RNA (ten nucleotides, orange), Rocaglamide A (RocA, red), and AMPPNP (not shown) (PDB code 5zc9). The interaction sites for the eIF4G MIF4G/HEAT1 domain are indicated in magenta as revealed by the complex structure in (A). (**C**) eIF4A interaction sites for the yeast eIF4G MIF4G/HEAT1 domain and the analogous putative ones for the human DAP5 MIF4G/HEAT1 domain are shown in magenta; for both proteins potential IRES interaction sites are shown in orange. IRES binding has been shown for human eIF4G and DAP5 MIF4G/HEAT1 domains and the indication of potential IRES binding sites is based on studies of human eIF4G. Loop$_{582–600}$ and Site 3 are illustrated as in (A). Residues of eIF4A interaction Site 3 are not resolved in the DAP5 MIF4G/HEAT1 domain crystal structure. In the potential IRES binding site of eIF4G, three residues (686–688) in Loop$_{677–691}$ are not resolved as indicated by the dashed line. In DAP5, this loop is fully resolved (Loop$_{142–161}$), where it adopts a different conformation than in eIF4G. (**D**) Structural surface characteristics of the MIF4G/HEAT1 domains of *S. cerevisiae* eIF4G (top six representations, PDB code 2vso) and human DAP5 (bottom six representations, PDB code 4iul). For both cases, the electrostatic surface potential, the surface hydrophobicity according to Kyte-Doolittle, and evolutionary conservation of surface residues are shown. The structures are shown in the same orientations as in (C).

There is a critical distinction between the nonspecific interactions of eIF4G with mRNA and the stronger and specific interactions with various IRESs. Single-molecule fluorescence assays and RIP-seq experiments indicate that eIF4G orthologs bind nonspecifically and dynamically with mRNA (163–165). In contrast, the interactions of eIF4G and DAP5 with IRESs are structure- and/or sequence-specific, suggesting that common structural folds in RNA could dictate the interactions (59,132,160,166–171). Thus, a protein with high affinity for a specific RNA sequence or structure motif may tend to have lower, albeit significant affinity for any RNA, and vice versa (56,172). The same is true for other eIFs. For example, eIF3 has high affinity for specific motifs in certain mRNAs, which plays an important role in translation reinitiation (173). Important for the present discussion, the helicase eIF4A also has high affinity for structures in some IRESs, where synergistic binding of eIF4A and eIF4G is critical for the high affinity and specificity of their binding to the IRES (168,174–176). Nonspecific RNA-binding proteins involved in translation initiation can thus have high affinity for specific RNA motifs, which may be used in the cell for regulation of translation (59,177–178). Deciphering the mechanisms of recognition of specific IRESs by DAP5 and eIF4G isoforms from different species, and the exact contact interfaces involved, would require solving the structures of a number of such complexes at high resolution.

To further tease apart the similarities and differences between the eIF4A and IRES interaction sites we analyzed protein surface features of the eIF4G and DAP5 MIF4G/HEAT1 domains (Figure 4D). We calculated electrostatic surface potentials by the Chimera Coulombic Electrostatics Plugin, surface hydrophobicity according to the Kyte-Doolittle scale, and analyzed evolutionary surface conservation employing the ConSurf algorithm (179–181). Our analyses of evolutionary surface conservation are based on alignments among 30 homologues, including the ones from *S. cerevisiae, C. albicans, C. elegans, A. thaliana, D. melanogaster, D. rerio, X. laevis, G. gallus, M. musculus, R. norvegicus, B. taurus, M. mulatta* and *H. sapiens*. At eIF4A interaction Sites 1 and 2, eIF4G and DAP5 exhibit similar surface signatures in charge distributions and hydrophobicity. Our analyses thus suggest that eIF4A binding may occur at these sites in DAP5. In particular, residues at both sites are evolutionarily highly conserved in eIF4G and DAP5. In contrast, the proposed IRES interaction site features different pattern in the two proteins. The negatively charged phosphates of the nucleic acid backbone are often involved in pairing with positively charged amino acid side chains of nucleic acid-binding proteins, even small differences of the electrostatic MIF4G/HEAT1 surface potentials are thus of particular relevance (182–186). Potentially, the observed variations provide a mechanistic basis for distinguishing between different IRESs, as both proteins have been shown to bind such RNA elements via their MIF4G/HEAT1 domains (59,109,132). Most interestingly, the proposed IRES interaction site appears to be less evolutionarily conserved in DAP5 than in eIF4G. We postulate that the afore-mentioned flexible loop at this site (Loop$_{677–691}$ in yeast eIF4G and Loop$_{142–161}$ in DAP5, see above and Figure 4C and D) may play an important role

for RNA binding mechanisms, for example by providing structural flexibility that enables recognition of different IRESs. Overall, the differences in surface features between the eIF4G and DAP5 MIF4G/HEAT1 domains, both from the vantage of electrostatics and evolutionary conservation are rather moderate. Achieving a better understanding how MIF4G/HEAT1 domains are involved in cap-dependent and IRES-dependent translation initiation and how they gain selectivity, demands further interaction studies especially with the RNA.

Interaction of W2/HEAT3 domains with eIF2β and MNK1/2

There are a number of occurrences of W2/HEAT3 domains among proteins involved in translation initiation and they mediate a multitude of interactions. The W2/HEAT3 domains of eIF4G and DAP5 bind to the MNK1/2 kinase while those of eIF5, eIF2Bε, and DAP5 mediate binding to eIF2β (Figure 3B). Multiple studies have suggested that the interaction of W2/HEAT3 with MNK1/2 is dictated by two specific and highly conserved motifs at the C-terminus of W2/HEAT3, which are composed of aromatic and acidic residues (AA box 1 and AA box 2) (Figure 5A) (68,187); AA box 2 is particularly important for functional interaction. MNK1/2 features a lysine/arginine-rich (KR) stretch in its N-terminal region that is proposed to mediate the interaction (Figure 5A) (188). This N-terminal segment of MNK1/2 is predicted to be unstructured and is distant from the catalytic domain, the nuclear export signal and the MAPK binding site, which are all located towards the C-terminus of MNK1/2. It is intriguing that a basic unstructured region serves as anchor to bind to the AA boxes on W2/HEAT3. Interestingly, the AA boxes are involved in binding of W2/HEAT3 to eIF2β as well, as shown by X-ray crystallography and nuclear magnetic resonance (NMR) binding studies (Figure 5A) (141,189). In its intrinsically disordered N-terminal tail, eIF2β features three lysine-rich sites (referred to as K-boxes; K1, K2 and K3), of which the K2 and K3 are suggested to have greater contribution to recognition of the AA boxes on W2/HEAT3. All three lysine motifs appear to be functionally important as demonstrated by *in vivo* studies, while K2 was reported to have a stronger contribution to binding to eIF5 *in vitro* (82,190). The K3 motif is sandwiched by segments that fold into α-helices (referred to as α-H^N and α-H^C), when bound to eIF5 W2/HEAT3 (Figure 5A) (189).

Molecular structures resolving interactions of either eIF4G, DAP5, eIF5 or eIF2Bε W2/HEAT3 with eIF2β or MNK1/2 are not available in databases. In the case of eIF4G–MNK1/2 binding, the KR region interacts predominantly with AA box 2, in particular with the intrinsically disordered portion of it (Arthanari, unpublished data). In a recent study, the yeast eIF2β−NTT K2-K3 region has been co-crystallized with eIF5 W2/HEAT3 (189); however, atomic coordinates have not been deposited in the Protein Data Bank. In this complex, K3 forms a loop contacting the eIF5 W2/HEAT3 domain via interactions of lysine side chains in K3 and residues in AA box 1 (Figure 5B), whereas K2 is disordered or dynamic as indicated by missing electron density in this study. Even in the folded K3
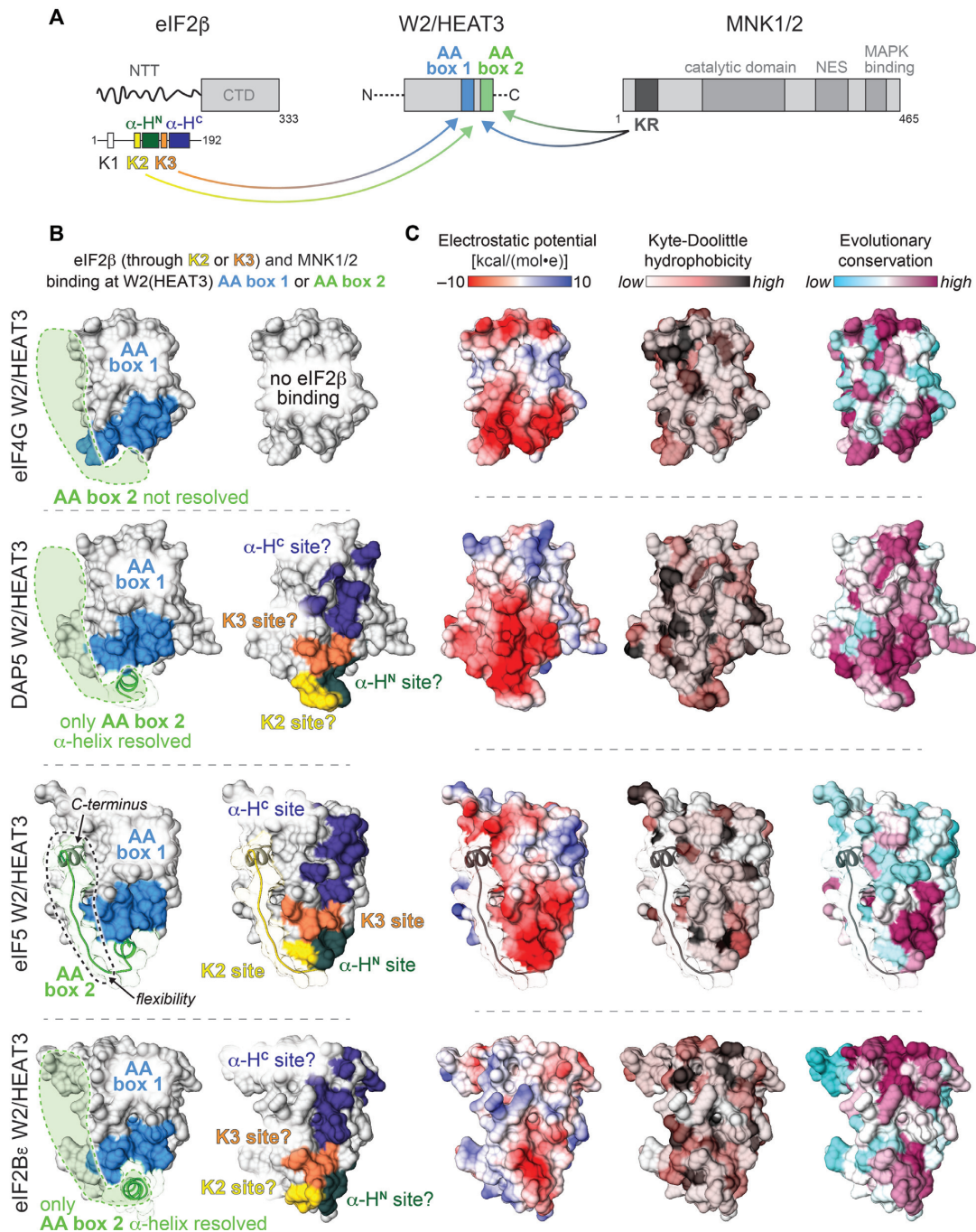
Figure 5. Interactions of eIF4G, DAP5, eIF5 and eIF2Bε W2/HEAT3 domains with eIF2β and MNK. (**A**) In the C-terminal region of W2/HEAT3, two sites composed of aromatic and acidic residues (AA box 1 (blue) and AA box 2 (green)) are proposed to mediate interactions to eIF2β and MNK stretches rich in lysine (K2 (yellow) and K3 (orange) motifs) and lysine/arginine (KR) residues, respectively. K1–K3 are located in the intrinsically disordered eIF2β N-terminal tail (NTT, residues 1–192). When bound to W2/HEAT3, the sequences N-terminal and C-terminal of the K3 motif fold into α-helices (α-H^N (dark green) and α-H^C (dark purple), respectively). In MNK, the KR stretch is close to the N-terminus; the catalytic domain, nuclear export signal (NES) and the MAPK binding site are located towards the MNK C-terminus. (**B**) AA box 1 and box 2 are shown in blue and green, respectively, for W2/HEAT3 domains of eIF4G (PDB code 1ug3), DAP5 (PDB code 3dm3), eIF5 (PDB code 2iu1) and eIF2Bε (PDB code 3jui). A structure of AA box 2 (shown in ribbon representation) is only fully resolved in the eIF5 crystal structure, where it adopts an α-helix at the N-terminus of AA box 2 and an extended loop. A second α-helix at the very C-terminus is not part of AA box 2, and the corresponding sequence is only present in metazoan eIF5. No electron density is observed for eIF4G AA box 2, and only partial structural information (for the N-terminal α-helix) is available for AA box 2 in DAP5 and eIF2Bε. Interaction sites with eIF2β K2 and K3 motifs, and the surrounding α-helices α-H^N and α-H^C in eIF2β are indicated by color-coded (according to (A)) surface representations on the W2/HEAT3 domain structures; experimental evidence at high resolution is only available for the interaction interfaces of eIF5 and eIF2β. (**C**) Structural surface characteristics of the W2/HEAT3 domains of eIF4G (PDB code 1ug3), DAP5 (PDB code 3dm3), eIF5 (PDB code 2iu1) and eIF2Bε (PDB code 3jui). The electrostatic surface potentials, the surface Kyte-Doolittle hydrophobicity, and evolutionary conservation of surface residues are shown. In these analyses, the loop and C-terminal α-helix in human eIF5 (depicted in ribbon representation) are not included as they are highly flexible in solution (191). All structures are shown in the same orientations as in (B).

motif, only a subset of the lysine side chains is resolved, suggesting they remain dynamic while still in the vicinity of the negatively charged AA boxes on the W2/HEAT3 surface. The strength of electrostatic interactions is dependent on the first power of distance, compared to the third or higher power of distance in other types of interactions; therefore, such dynamic contacts could be entropically favorable. Remarkably, the crystal structure of the eIF2β-NTT:eIF5 W2/HEAT3 complex shows that the eIF2β segments surrounding K3 fold into the two α-helices α-H^N and α-H^C, and play a major role by contributing to the binding free energy through hydrophobic interactions [189]. In fact, α-H^N and α-H^C position K3 (and possibly K2) in the vicinity of the AA boxes on the eIF5 surface. These α-helical segments are as conserved as the K motifs but have not received as much attention so far. While eIF2β K2 was not resolved in the crystal structure, the authors proposed that K2 could be interacting with the negatively charged surface formed by AA boxes 1 and 2 of eIF5 [189]. In good agreement with this study, mutational analysis [82,83] and NMR studies [141,191] have shown that AA box 2 plays a central role in the eIF5–eIF2β interaction. In mammals, phosphorylation of the AA box 2 in eIF5 by Casein Kinase 2 (CK2) promotes protein synthesis and cell proliferation [192], mediated by increasing the eIF5 affinity for eIF2β [191]. Recently, the complex of eIF2 and eIF2B has been studied by cryo-electron microscopy, but the eIF2β−NTT could not be resolved [125,140]. Based on the crystallography and NMR results, we charted the interaction sites for eIF2β binding through K2, K3, and the adjoining α-helices α-H^N and α-H^C onto the surface of the DAP5, eIF5 and eIF2Bε W2/HEAT3 domains (Figure 5B) (eIF4G does not interact with eIF2β, see Figure 3B). This highlights involvement of W2/HEAT3 AA box 1 residues in binding of the K3 motif and to a smaller extent of K2, α-H^N and α-H^C. Presumably, AA box 2 is mainly involved in an interaction with K2. It is worth noting that experimental evidence for eIF2β−NTT binding sites is available only for eIF5; however, a number of W2/HEAT3 residues at these sites are conserved among DAP5, eIF5, and eIF2Bε. Among the crystal structures available for the eIF4G, DAP5, eIF5, and eIF2Bε W2/HEAT3 domains, AA box 2, located at the very C-terminus, is visible only in the case of eIF5 (Figure 5B) [84]. AA box 2 establishes an extended loop that folds back on the eIF5 W2/HEAT3 surface. However, NMR data indicate that even in eIF5, AA box 2 is disordered in solution and only dynamically contacts the W2/HEAT3 surface [191]. Combined with the missing electron density in the other three W2/HEAT3 domain structures, this suggests high flexibility of this region in AA box 2. The short α-helix of AA box 2 resolved in DAP5, eIF5, and eIF2Bε W2/HEAT3 overlaps well with the proposed eIF2β K2 motif binding site and participates in the binding interface to α-H^N, whereas, as described above, eIF2β K3 contacts a portion of AA box 1 [189].

To evaluate if surface characteristics of the W2/HEAT3 domains help to understand why eIF4G W2/HEAT3 does not bind eIF2β, why eIF5 and eIF2Bε do not bind MNK1/2, and why DAP5 W2/HEAT3 binds both eIF2β and MNK1/2, we analyzed again the surface electrostatic potentials, hydrophobicity, and evolutionary conservation

of the four W2/HEAT3 domains as we have done earlier for the case of MIF4G/HEAT1 (Figure 5C). First, AA box 1 constitutes a pronounced negatively charged area in all four W2/HEAT3 domains; however, to a lesser extent in the case of eIF2Bε. This may be compensated by negatively charged residues in AA box 2, which is only partially resolved in eIF2Bε. However, we did not include AA box 2 in surface characteristics analyses and comparison among the proteins since electron density for this region is only observed for eIF5 (a large portion of the eIF5 AA box 2 surface is negatively charged). No major variations in hydrophobicity are observed between the four W2/HEAT3 domain surfaces. As expected, the α-H^N and α-H^C binding sites in DAP5, eIF5, and eIF2Bε feature hydrophobic residues. These residues might be functionally relevant as protein–protein interactions are often mainly driven by hydrophobic interactions [185]. The distinctive electrostatic signature in AA box 1 is clearly noticeable, and a significant part of it is well-conserved in all four proteins (Figure 5C). A second negative patch on eIF4G W2/HEAT3 is conserved as well, and the W2/HEAT3 domains of DAP5 and eIF2Bε have additional conserved sites. In the case of DAP5, it is rather positively charged, and in eIF2Bε this second conserved area is of rather hydrophobic nature, consistent with it being the contact surface for eIF2γ [139,140]. While the AA boxes are well-conserved among eIF4G, DAP5, eIF5, and eIF2Bε, other surface areas are not as universally conserved. Therefore, a likely reason for why eIF4G does not interact with eIF2β is that the surface area, which in eIF5 used to engage the α-helices surrounding eIF2β-K3, is not conserved between eIF5 and eIF4G. This idea is supported by the observation that eIF4G binding to MNK1/2 involves predominantly the AA box 2 [188].

The C-terminal AA box 2 may only transiently fold back on W2/HEAT3 (as seen in eIF5) and may populate multiple conformational states of which each can promote binding to specific interaction partners [191]. Future investigations are required to decipher if this transient nature is key for how the eIF4G, DAP5, eIF5 and eIF2Bε W2/HEAT3 domains selectively interact with their binding partners. Here, NMR can be used to identify transient and minor conformations. Especially as AA box 2 has been suggested to be mainly responsible for eIF4G/DAP5–MNK1/2 binding [188], analyses of structural plasticity, including detailed studies of the interactions, are expected to provide important insight into molecular mechanisms of W2/HEAT3 domains in translation initiation.

OPEN QUESTIONS AND CONCLUDING THOUGHTS

Though HEAT domains are known to orchestrate a diverse array of cellular functions, the abundance of HEAT domains in translation initiation is striking. As discussed above, the HEAT domains of translation initiation factors can be classified into three distinct categories, MIF4G/HEAT1, MA3/HEAT2 and W2/HEAT3, based on a combination of structural, sequence, and functional properties. By analyzing four specific initiation factors of eukaryotic translation, eIF4G, DAP5, eIF5 and eIF2Bε, we highlight the importance of these HEAT domains in

translation initiation. Even though a structure comparison provides only limited insight, investigating structural signatures through surface analyses — electrostatic potential, hydrophobicity, evolutionary conservation, and binding studies — reveals some potentially important differences among the HEAT domains of these four proteins. As HEAT domains have high structural but low sequence similarities, variations in biochemical properties, in particular in flexible regions, may conceptualize basic principles to mediate the multitude of protein–protein and protein–nucleic acid interactions. The large amount of work on HEAT domains accomplished since their discovery in 1995 impressively revealed their fundamental role in cellular functions including protein synthesis (1,3,17,43,58).

Despite a large body of available structural information and biophysical and interaction data on the HEAT domains, there are several open questions. To further understand protein–protein interactions involving eIF4G, DAP5, eIF5 and eIF2Bε mediated by their HEAT domains, we suggest that detailed studies of flexible regions, i.e. $Loop_{582-600}$ in MIF4G/HEAT1 and AA box 2 in W2/HEAT3, have to be performed. Of the three types of HEAT domains, the AA boxes are exclusive to the W2/HEAT3 domain. These AA boxes often engage in interactions with intrinsically disordered regions; in fact, W2/HEAT3 domains often interact with IDRs containing basic residues.

In addition, high-resolution studies of MIF4G/HEAT1–RNA interactions are required to better understand noncanonical translation initiation mechanisms. A molecular structure of a viral IRES and interaction studies with the MIF4G/HEAT1 domain of eIF4G indicate binding mediated by π–π stacking involving adenosine and aromatic amino acid side chains (59). Are there specific RNA structures with common characteristics that are recognized by HEAT domains? Towards establishing general concepts of how HEAT domains bind RNA, more of such interaction studies at atomic resolution are needed.

Most of the reported interactions involving the HEAT domains in translation initiation are in the low micromolar range, including binding of MIF4G/HEAT1 domains to viral components such as the encephalomyocarditis virus IRES or the murine norovirus VPg protein, which contribute to regulation of translation in the context of viral replication (Table 1). This begs the question whether low affinity interaction is a distinct feature of HEAT domains involved in translation initiation which requires transient, yet critical interaction, or whether the interactions measured in isolated contexts do not capture the actual binding affinity. In case of interactions involving IDRs, it has been shown for other systems that avidity-based interactions increase the binding affinity, and it is well conceivable that using full-length constructs and additional components of the translation initiation machinery are necessary to observe more physiologically relevant affinities.

Beyond the idea of analyzing differences in HEAT domains to identify molecular mechanisms, more work is needed to further understand the remarkable functional versatility of HEAT domains and the proteins in which they are encountered. Specifically, it is intriguing that several HEAT domain-containing proteins feature IDRs around these domains. As suggested by Yoshimura and Hirano,

proteins with HEAT domains can be classified into three groups: one, 'HEAT only', two, 'HEAT with IDRs', and three, 'HEAT with other functional domain(s)' (2). Following this idea, it is unconditionally required to study the impact of IDRs on the various functions of HEAT domain-containing proteins in the second group of this classification, which includes eIF4G, DAP5, eIF5, and eIF2Bε. As we show, short, disordered regions flanking the MIF4G/HEAT1 and W2/HEAT3 domains are functionally highly relevant in these four proteins. To further understand their complex protein–protein and protein–nucleic acid interactions, we think comprehensive studies of the extended IDRs that link HEAT domains are required. Given the remarkable structural flexibility HEAT domains exhibit, the even more flexible IDRs may establish an additional layer of complexity to accomplish protein function and control of the respective cellular processes (193–195). For example, these IDRs could mediate secondary interactions, especially with RNA, and potentially play a role as spacer providing separation between docking modules and functional sites. These would include avidity-based interactions driven by binding of the structured part of the HEAT domain and the IDRs would provide additional engagement. These IDRs harbor several phosphorylation sites and the contribution to the binding affinity by the IDRs can be further modulated by phosphorylation events. This is especially significant in the case of HEAT domain interactions with RNA, where electrostatics play an important role. IDRs could also act as conduits connecting multiple proteins and bringing proteins and RNA together, which is a common theme in translation initiation. IDRs are also known to undergo disorder-order transitions upon engaging an interaction partner, another modality that a scaffold protein such as the HEAT domain proteins in translation initiation can employ to nucleate interaction hubs. The role of IDRs in the HEAT domain-containing translation proteins demands further studies. Evolutionary sequence conservation correlation can provide good starting points for such investigation. Employing the powerful methods that have been established in recent years to study IDRs, most importantly NMR spectroscopy, small angle X-ray scattering and (single molecule) fluorescence spectroscopy techniques, could shed light onto structural determinants of the IDR-mediated interactions (196–199). With the recent developments in de novo structure prediction/determination, we were curious to find any possible interaction between HEAT domains and between the IDRs and the HEAT domain in the structures of full-length proteins. We analyzed the structures of full-length eIF4G, DAP5, eIF5 and eIF2Be predicted by the recently introduced artificial intelligence-based program AlphaFold (200,201). For the above proteins, there was no additional information or novel interactions in the AlphaFold structures that can be gleaned with high confidence. This does not mean that there are no interactions, especially considering the fact that some of the interactions between the IDRs and structured domain, though vital, are weak in terms of interaction thermodynamics but are often stabilized by avidity and transient in nature. It is well-known that IDRs sample a large conformational space contradicting the notion of a single globular structure of these proteins. Thus, the question of the

Table 1. HEAT domains of translation initiation factors typically interact in the low μM affinity range with binding partners

Domain	Protein	Interaction partner	K_d [μM]	Method	Reference
MIF4G/HEAT1	eIF4GI	EMCV IRES (RNA)	1.3	ITC	(59)
	eIF4GI	eIF4A	0.14	ITC	(127)
	DAP5	eIF4A	1.1	ITC	(127)
	eIF4G	eIF4A	12.1	SPR	(61)
	eIF4GII	MNV VPg (1–124)	5.2	ITC	(60)
	eIF4GI	MNV VPg (104–124)	3.0	FA	(60)
	DAP5	MNV VPg (104–124)	20.0	FA	(60)
MA3/HEAT2	eIF4GI	eIF4A	1.1	SPR	(61)
	eIF4GI	eIF4A	0.9	ITC	(61)
W2/HEAT3	eIF5	eIF2β-K2K3	∼ 4	ITC	(141)
	eIF5	eIF2β-NTD	∼ 17	ITC	(141)

For the three classes MIF4G/HEAT1, MA3/HEAT2 and W2/HEAT3, affinities for a number of interactions with binding partners have been determined by isothermal titration calorimetry (ITC), surface plasmon resonance (SPR) and fluorescence anisotropy (FA). EMCV = Encephalomyocarditis Virus; MNV = Murine Norovirus; VPg = Virus Protein, genome-linked; NTD = N-terminal domain.

interplay between IDRs and HEAT domains still remains at large.

Recently, IDRs have been implicated in activity-dependent translation, especially in neurons facilitating synaptic plasticity and long-term memory (202). Here, the mRNA is maintained in a translationally dormant form in membrane-less protein assemblies known as neuronal granules formed by a phenomenon referred to as liquid-liquid phase separation. This phase separation is driven by the C-terminal IDR of the RNA-binding protein Fragile X Mental Retardation Protein (FMRP), abundantly found in neuronal granules (202). Post-translational modifications seem to regulate the IDR-mediated phase separation, thus enabling translation in response to a stimulus. The IDRs sandwiching the HEAT domains could be involved in similar mechanisms providing an additional regulatory mechanism to on-demand translation of select mRNAs. Phase separation has also been linked to cation–π interactions, which may play a role in recognition of RNAs by IDRs of HEAT domain-containing proteins in addition to π–π interactions (203).

To better understand the structural and mechanistic underpinnings of HEAT domain-containing protein function, focus should further reside in investigating interactions and macromolecular complexes both with proteins and nucleic acids. Understanding structural plasticity and/or dynamics of these HEAT domains at atomic level and the interplay with post-translational modifications (for the sites found in IDRs flanking the HEAT domains) will lead to a better understanding of the multitude of functions orchestrated by the HEAT domains. It is established that phosphorylation can critically regulate the disorder–structure relationship in proteins (194,204–206). As an example, studying the IDR of approximately 240 residues between the MIF4G/HEAT1 and MA3/HEAT2 domains of DAP5 seems to be a promising starting point for such investigations (Figure 3A). In this region of DAP5, four different phosphorylation sites have been identified and verified experimentally (207–209), and we expect that characterizing how these sites affect DAP5 structure and function through biophysical methods will exemplify the relevance of phosphorylation in IDRs that flank HEAT domains of eukaryotic translation initiation factors.

Though HEAT domains are structurally similar, through their meticulously evolved sequence composition and structural plasticity they function as swiss army knife in translation initiation, forging multiple specific interactions. Even though binding affinities of these interactions are moderate, in the low micromolar range, they are critical in control of translation initiation, which requires several transient interactions, remodeling of the complex and frequent dissociation of proteins. A well-documented example of such an interaction is the binding of MIF4G/HEAT1 domains with eIF4A and RNA as discussed above. Thus, some of the protein–protein interactions involving HEAT domains represent promising therapeutic targets.

DATA AVAILABILITY

All structures that were analyzed in this article can be accessed via the Protein Data Bank. Relevant PDB IDs are mentioned in the respective figure legends. Any data from our analyses described in this article is available from the authors upon request.

REFERENCES

1. Andrade,M.A. and Bork,P. (1995) HEAT repeats in the Huntington's disease protein. *Nat. Genet.*, **11**, 115–116.
2. Yoshimura,S.H. and Hirano,T. (2016) HEAT repeats – versatile arrays of amphiphilic helices working in crowded environments? *J. Cell Sci.*, **129**, 3963–3970.

3. Neuwald,A.F. and Hirano,T. (2000) HEAT repeats associated with condensins, cohesins, and other complexes involved in chromosome-related functions. *Genome Res.*, **10**, 1445–1452.

4. Groves,M.R. and Barford,D. (1999) Topological characteristics of helical repeat proteins. *Curr. Opin. Struct. Biol.*, **9**, 383–389.

5. Choe,J., Kelker,M.S. and Wilson,I.A. (2005) Crystal structure of Human Toll-Like Receptor 3 (TLR3) Ectodomain. *Science*, **309**, 581–585.

6. Kobe,B. and Deisenhofer,J. (1993) Crystal structure of porcine ribonuclease inhibitor, a protein with leucine-rich repeats. *Nature*, **366**, 751–756.

7. Krieger,I., Kostyukova,A., Yamashita,A., Nitanai,Y. and Maéda,Y. (2002) Crystal structure of the C-Terminal half of tropomodulin and structural basis of actin filament pointed-end capping. *Biophys. J.*, **83**, 2716–2725.

8. Huber,A.H., Nelson,W.J. and Weis,W.I. (1997) Three-Dimensional structure of the armadillo repeat region of β-Catenin. *Cell*, **90**, 871–882.

9. Goldfarb,D.S., Corbett,A.H., Mason,D.A., Harreman,M.T. and Adam,S.A. (2004) Importin alpha: a multipurpose nuclear-transport receptor. *Trends Cell Biol.*, **14**, 505–514.

10. Fontes,M.R., Teh,T. and Kobe,B. (2000) Structural basis of recognition of monopartite and bipartite nuclear localization sequences by mammalian importin-alpha. *J. Mol. Biol.*, **297**, 1183–1194.

11. Conti,E., Uy,M., Leighton,L., Blobel,G. and Kuriyan,J. (1998) Crystallographic analysis of the recognition of a nuclear localization signal by the nuclear import factor karyopherin α. *Cell*, **94**, 193–204.

12. Breeden,L. and Nasmyth,K. (1987) Similarity between cell-cycle genes of budding yeast and fission yeast and the Notch gene of Drosophila. *Nature*, **329**, 651–654.

13. Lux,S.E., John,K.M. and Bennett,V. (1990) Analysis of cDNA for human erythrocyte ankyrin indicates a repeated structure with homology to tissue-differentiation and cell-cycle control proteins. *Nature*, **344**, 36–42.

14. Grinthal,A., Adamovic,I., Weiner,B., Karplus,M. and Kleckner,N. (2010) PR65, the HEAT-repeat scaffold of phosphatase PP2A, is an elastic connector that links force and catalysis. *Proc. Natl. Acad. Sci. USA*, **107**, 2467–2472.

15. Stewart,M. (2007) Molecular mechanism of the nuclear protein import cycle. *Nat. Rev. Mol. Cell Biol.*, **8**, 195–208.

16. Andrade,M.A., Petosa,C., O'Donoghue,S.I., Müller,C.W. and Bork,P. (2001) Comparison of ARM and HEAT protein repeats. *J. Mol. Biol.*, **309**, 1–18.

17. Forwood,J.K., Lange,A., Zachariae,U., Marfori,M., Preast,C., Grubmuller,H., Stewart,M., Corbett,A.H. and Kobe,B. (2010) Quantitative structural analysis of importin-β flexibility: paradigm for solenoid protein structures. *Structure*, **18**, 1171–1183.

18. Tsytlonok,M., Craig,P.O., Sivertsson,E., Serquera,D., Perrett,S., Best,R.B., Wolynes,P.G. and Itzhaki,L.S. (2013) Complex energy landscape of a giant repeat protein. *Structure*, **21**, 1954–1965.

19. Kappel,C., Zachariae,U., Dölker,N. and Grubmüller,H. (2010) An unusual hydrophobic core confers extreme flexibility to HEAT repeat proteins. *Biophys. J.*, **99**, 1596–1603.

20. Conti,E. and Izaurralde,E. (2001) Nucleocytoplasmic transport enters the atomic age. *Curr. Opin. Cell Biol.*, **13**, 310–319.

21. Li,Y., Muir,K.W., Bowler,M.W., Metz,J., Haering,C.H. and Panne,D. (2018) Structural basis for Scc3-dependent cohesin recruitment to chromatin. *Elife*, **7**, e38356.

22. Conti,E., Müller,C.W. and Stewart,M. (2006) Karyopherin flexibility in nucleocytoplasmic transport. *Curr. Opin. Struct. Biol.*, **16**, 237–244.

23. Lee,S.J., Imamoto,N., Sakai,H., Nakagawa,A., Kose,S., Koike,M., Yamamoto,M., Kumasaka,T., Yoneda,Y. and Tsukihara,T. (2000) The adoption of a twisted structure of importin-β is essential for the protein-protein interaction required for nuclear transport. *J. Mol. Biol.*, **302**, 251–264.

24. Rubinson,E.H. and Eichman,B.F. (2012) Nucleic acid recognition by tandem helical repeats. *Curr. Opin. Struct. Biol.*, **22**, 101–109.

25. Stein,A.J., Fuchs,G., Fu,C., Wolin,S.L. and Reinisch,K.M. (2005) Structural insights into RNA quality control: the ro autoantigen binds misfolded RNAs via its central cavity. *Cell*, **121**, 529–539.

26. Walker,F.O. (2007) Huntington's disease. *Lancet*, **369**, 218–228.

27. Masahisa,K., Haruhiko,B., Keisuke,S., Yu,T., Motoshi,K., Fumiaki,T., Hiroaki,A. and Gen,S. (2008) Molecular genetics and biomarkers of polyglutamine diseases. *Curr. Mol. Med.*, **8**, 221–234.

28. Skogerson,L. and Engelhardt,D. (1977) Dissimilarity in protein chain elongation factor requirements between yeast and rat liver ribosomes. *J. Biol. Chem.*, **252**, 1471–1475.

29. Chakraburtty,K. and Kamath,A. (1988) Protein synthesis in yeast. *Int. J. Biochem.*, **20**, 581–590.

30. Kamath,A. and Chakraburtty,K. (1989) Role of yeast elongation factor 3 in the elongation cycle. *J. Biol. Chem.*, **264**, 15423–15428.

31. Cho,U.S. and Xu,W. (2007) Crystal structure of a protein phosphatase 2A heterotrimeric holoenzyme. *Nature*, **445**, 53–57.

32. Groves,M.R., Hanlon,N., Turowski,P., Hemmings,B.A. and Barford,D. (1999) The structure of the protein phosphatase 2A PR65/A subunit reveals the conformation of its 15 tandemly repeated HEAT motifs. *Cell*, **96**, 99–110.

33. Lin,X.H., Walter,J., Scheidtmann,K., Ohst,K., Newport,J. and Walter,G. (1998) Protein phosphatase 2A is required for the initiation of chromosomal DNA replication. *Proc. Natl. Acad. Sci. USA*, **95**, 14693–14698.

34. Depaoli-Roach,A.A., Park,I.-K., Cerovsky,V., Csortos,C., Durbin,S.D., Kuntz,M.J., Sitikov,A., Tang,P.M., Verin,A. and Zolnierowicz,S. (1994) Serine/threonine protein phosphatases in the control of cell function. *Adv. Enzym. Regul.*, **34**, 199–224.

35. Sontag,E. (2001) Protein phosphatase 2A: the Trojan Horse of cellular signaling. *Cell. Signal.*, **13**, 7–16.

36. Chao,L. and Avruch,J. (2019) Cryo-EM insight into the structure of MTOR complex 1 and its interactions with Rheb and substrates. *F1000Research*, **8**, 1–10.

37. Yang,H., Chen,X., Liu,M. and Xu,Y. (2018) The structure of mTOR complexes at a glance. *Precis. Cancer Med.*, **1**, 7.

38. Aylett,C.H.S., Sauer,E., Imseng,S., Boehringer,D., Hall,M.N., Ban,N. and Maier,T. (2015) Architecture of human mTOR complex 1. *Science*, **351**, 48–52.

39. Sabatini,D.M. (2017) Twenty-five years of mTOR: uncovering the link from nutrients to growth. *Proc. Natl. Acad. Sci. USA*, **114**, 11818–11825.

40. Laplante,M. and Sabatini,D.M. (2012) mTOR signaling in growth control and disease. *Cell*, **149**, 274–293.

41. Mossmann,D., Park,S. and Hall,M.N. (2018) mTOR signalling and cellular metabolism are mutual determinants in cancer. *Nat. Rev. Cancer*, **18**, 744–757.

42. Saxton,R.A. and Sabatini,D.M. (2017) mTOR signaling in growth, metabolism, and disease. *Cell*, **168**, 960–976.

43. Perry,J. and Kleckner,N. (2003) The ATRs, ATMs, and TORs are giant HEAT repeat proteins. *Cell*, **112**, 151–155.

44. Lee,S.J., Matsuura,Y., Liu,S.M. and Stewart,M. (2005) Structural basis for nuclear import complex dissociation by RanGTP. *Nature*, **435**, 693–696.

45. Mackmull,M.-T., Klaus,B., Heinze,I., Chokkalingam,M., Beyer,A., Russell,R.B., Ori,A. and Beck,M. (2017) Landscape of nuclear transport receptor cargo specificity. *Mol. Syst. Biol.*, **13**, 962–962.

46. Hampoelz,B., Andres-Pons,A., Kastritis,P. and Beck,M. (2019) Structure and assembly of the nuclear pore complex. *Annu. Rev. Biophys.*, **48**, 515–536.

47. Cautain,B., Hill,R., de Pedro,N. and Link,W. (2015) Components and regulation of nuclear transport processes. *The FEBS J.*, **282**, 445–462.

48. Beck,M. and Hurt,E. (2017) The nuclear pore complex: understanding its function through structural insight. *Nat. Rev. Mol. Cell Biol.*, **18**, 73–89.

49. Vetter,I.R., Arndt,A., Kutay,U., Görlich,D. and Wittinghofer,A. (1999) Structural view of the ran–importin β interaction at 2.3 Å resolution. *Cell*, **97**, 635–646.

50. Garces,R.G., Gillon,W. and Pai,E.F. (2007) Atomic model of human Rcd-1 reveals an armadillo-like-repeat protein with in vitro nucleic acid binding properties. *Protein Sci.*, **16**, 176–188.

51. Green,C.D., Long,K.S., Shi,H. and Wolin,S.L. (1998) Binding of the 60-kDa Ro autoantigen to Y RNAs: evidence for recognition in the major groove of a conserved helix. *RNA*, **4**, 750–765.

52. Hall,A.E., Turnbull,C. and Dalmay,T. (2013) Y RNAs: recent developments. *BioMol. Concepts*, **4**, 103–110.

53. Reinisch,K.M. and Wolin,S.L. (2007) Emerging themes in non-coding RNA quality control. *Curr. Opin. Struct. Biol.*, **17**, 209–214.

54. Chen,X. and Wolin,S.L. (2004) The Ro 60 kDa autoantigen: insights into cellular function and role in autoimmunity. *J. Mol. Med.*, **82**, 232–239.

55. Ponting,C.P. (2000) Novel eIF4G domain homologues linking mRNA translation with nonsense-mediated mRNA decay. *Trends Biochem. Sci.*, **25**, 423–426.

56. Marintchev,A. and Wagner,G. (2005) Translation initiation: structures, mechanisms and evolution. *Q. Rev. Biophys.*, **37**, 197–284.

57. Boesen,T., Mohammad,S.S., Pavitt,G.D. and Andersen,G.R. (2004) Structure of the catalytic fragment of translation initiation factor 2B and identification of a critically important catalytic residue. *J. Biol. Chem.*, **279**, 10584–10592.

58. Marcotrigiano,J., Lomakin,I.B., Sonenberg,N., Pestova,T.V., Hellen,C.U.T. and Burley,S.K. (2001) A conserved HEAT domain within eIF4G directs assembly of the translation initiation machinery. *Mol. Cell*, **7**, 193–203.

59. Imai,S., Kumar,P., Hellen,C.U.T., D'Souza,V.M. and Wagner,G. (2016) An accurately preorganized IRES RNA structure enables eIF4G capture for initiation of viral translation. *Nat. Struct. Mol. Biol.*, **23**, 859–864.

60. Leen,E.N., Sorgeloos,F., Correia,S., Chaudhry,Y., Cannac,F., Pastore,C., Xu,Y., Graham,S.C., Matthews,S.J., Goodfellow,I.G. *et al.* (2016) A conserved interaction between a C-Terminal motif in norovirus VPg and the HEAT-1 domain of eIF4G is essential for translation initiation. *PLoS Pathog.*, **12**, e1005379.

61. Marintchev,A., Edmonds,K.A., Marintcheva,B., Hendrickson,E., Oberer,M., Suzuki,C., Herdy,B., Sonenberg,N. and Wagner,G. (2009) Topology and regulation of the human eIF4A/4G/4H helicase complex in translation initiation. *Cell*, **136**, 447–460.

62. Kim,K.M., Cho,H., Choi,K., Kim,J., Kim,B.-W., Ko,Y.-G., Jang,S.K. and Kim,Y.K. (2009) A new MIF4G domain-containing protein, CTIF, directs nuclear cap-binding protein CBP80/20-dependent translation. *Genes Dev.*, **23**, 2033–2045.

63. Cakmakci,N.G., Lerner,R.S., Wagner,E.J., Zheng,L. and Marzluff,W.F. (2008) SLIP1, a factor required for activation of histone mRNA translation by the stem-loop binding protein. *Mol. Cell. Biol.*, **28**, 1182–1194.

64. Hernández,G., Miron,M., Han,H., Liu,N., Magescas,J., Tettweiler,G., Frank,F., Siddiqui,N., Sonenberg,N. and Lasko,P. (2013) Mextli is a novel eukaryotic translation initiation factor 4E-Binding protein that promotes translation in drosophila melanogaster. *Mol. Cell. Biol.*, **33**, 2854–2864.

65. Clerici,M., Deniaud,A., Boehm,V., Gehring,N.H., Schaffitzel,C. and Cusack,S. (2013) Structural and functional analysis of the three MIF4G domains of nonsense-mediated decay factor UPF2. *Nucleic Acids Res.*, **42**, 2673–2686.

66. Palacios,I.M., Gatfield,D., St Johnston,D. and Izaurralde,E. (2004) An eIF4AIII-containing complex required for mRNA localization and nonsense-mediated mRNA decay. *Nature*, **427**, 753–757.

67. Andersen,C.B.F., Ballut,L., Johansen,J.S., Chamieh,H., Nielsen,K.H., Oliveira,C.L.P., Pedersen,J.S., Séraphin,B., Hir,H.L. and Andersen,G.R. (2006) Structure of the exon junction core complex with a trapped DEAD-Box ATPase bound to RNA. *Science*, **313**, 1968–1972.

68. Bellsolell,L., Cho-Park,P.F., Poulin,F., Sonenberg,N. and Burley,S.K. (2006) Two structurally atypical HEAT domains in the C-Terminal portion of human eIF4G support binding to eIF4A and mnk1. *Structure*, **14**, 913–923.

69. Imataka,H. and Sonenberg,N. (1997) Human eukaryotic translation initiation factor 4G (eIF4G) possesses two separate and independent binding sites for eIF4A. *Mol. Cell. Biol.*, **17**, 6940–6947.

70. Lamphear,B.J., Kirchweger,R., Skern,T. and Rhoads,R.E. (1995) Mapping of functional domains in eukaryotic protein synthesis initiation factor 4G (eIF4G) with picornaviral proteases: implications for cap-dependent and cap-independent translational initiation. *J. Biol. Chem.*, **270**, 21975–21983.

71. Phillips,S.E.V. (2006) Turning up the HEAT on translation. *Structure*, **14**, 806–807.

72. Simmons,H.M., Ruis,B.L., Kapoor,M., Hudacek,A.W. and Conklin,K.F. (2005) Identification of NOM1, a nucleolar, eIF4A binding protein encoded within the chromosome 7q36 breakpoint region targeted in cases of pediatric acute myeloid leukemia. *Gene*, **347**, 137–145.

73. Imataka,H., Olsen,H.S. and Sonenberg,N. (1997) A new translational regulator with homology to eukaryotic translation initiation factor 4G. *EMBO J.*, **16**, 817–825.

74. Levy-Strumpf,N., Deiss,L.P., Berissi,H. and Kimchi,A. (1997) DAP-5, a novel homolog of eukaryotic translation initiation factor 4G isolated as a putative modulator of gamma interferon-induced programmed cell death. *Mol. Cell. Biol.*, **17**, 1615–1625.

75. Shaughnessy,J.D., Jenkins,N.A. and Copeland,N.G. (1997) cDNA cloning, expression analysis, and chromosomal localization of a gene with high homology to wheat eIF-(iso)4F and mammalian eIF-4G. *Genomics*, **39**, 192–197.

76. Yamanaka,S., Poksay,K.S., Arnold,K.S. and Innerarity,T.L. (1997) A novel translational repressor mRNA is edited extensively in livers containing tumors caused by the transgene expression of the apoB mRNA-editing enzyme. *Genes Dev.*, **11**, 321–333.

77. Shibahara,K., Asano,M., Ishida,Y., Aoki,T., Koike,T. and Honjo,T. (1995) Isolation of a novel mouse gene MA-3 that is induced upon programmed cell death. *Gene*, **166**, 297–301.

78. Suzuki,C., Garces,R.G., Edmonds,K.A., Hiller,S., Hyberts,S.G., Marintchev,A. and Wagner,G. (2008) PDCD4 inhibits translation initiation by binding to eIF4A using both its MA3 domains. *Proc. Natl. Acad. Sci. USA*, **105**, 3274–3279.

79. Marintchev,A. and Wagner,G. (2005) eIF4G and CBP80 share a common origin and similar domain organization: implications for the structure and function of eIF4G. *Biochemistry*, **44**, 12265–12272.

80. Moura,D.M.N., Reis,C.R.S., Xavier,C.C., da Costa Lima,T.D., Lima,R.P., Carrington,M. and de Melo Neto,O.P. (2015) Two related trypanosomatid eIF4G homologues have functional differences compatible with distinct roles during translation initiation. *RNA Biol.*, **12**, 305–319.

81. Singh,C.R., Watanabe,R., Zhou,D., Jennings,M.D., Fukao,A., Lee,B., Ikeda,Y., Chiorini,J.A., Campbell,S.G., Ashe,M.P. *et al.* (2011) Mechanisms of translational regulation by a human eIF5-mimic protein. *Nucleic Acids Res.*, **39**, 8314–8328.

82. Asano,K., Krishnamoorthy,T., Phan,L., Pavitt,G.D. and Hinnebusch,A.G. (1999) Conserved bipartite motifs in yeast eIF5 and eIF2Bε, GTPase-activating and GDP–GTP exchange factors in translation initiation, mediate binding to their common substrate eIF2. *EMBO J.*, **18**, 1673–1688.

83. Yamamoto,Y., Singh,C.R., Marintchev,A., Hall,N.S., Hannig,E.M., Wagner,G. and Asano,K. (2005) The eukaryotic initiation factor (eIF) 5 HEAT domain mediates multifactor assembly and scanning with distinct interfaces to eIF1, eIF2, eIF3, and eIF4G. *Proc. Natl. Acad. Sci. USA*, **102**, 16164–16169.

84. Bieniossek,C., Schütz,P., Bumann,M., Limacher,A., Uson,I. and Baumann,U. (2006) The crystal structure of the carboxy-terminal domain of human translation initiation factor eIF5. *J. Mol. Biol.*, **360**, 457–465.

85. Asano,K., Shalev,A., Phan,L., Nielsen,K., Clayton,J., Valášek,L., Donahue,T.F. and Hinnebusch,A.G. (2001) Multiple roles for the C-terminal domain of eIF5 in translation initiation complex assembly and GTPase activation. *EMBO J.*, **20**, 2326–2337.

86. Liberman,N., Dym,O., Unger,T., Albeck,S., Peleg,Y., Jacobovitch,Y., Branzburg,A., Eisenstein,M., Marash,L. and Kimchi,A. (2008) The crystal structure of the C-Terminal DAP5/p97 domain sheds light on the molecular basis for its processing by caspase cleavage. *J. Mol. Biol.*, **383**, 539–548.

87. Marton,M.J., Crouch,D. and Hinnebusch,A.G. (1993) GCN1, a translational activator of GCN4 in saccharomyces cerevisiae, is required for phosphorylation of eukaryotic translation initiation factor 2 by protein kinase GCN2. *Mol. Cell. Biol.*, **13**, 3541–3556.

88. Castilho,B.A., Shanmugam,R., Silva,R.C., Ramesh,R., Himme,B.M. and Sattlegger,E. (2014) Keeping the eIF2 alpha kinase Gcn2 in check. *Biochim. Biophys. Acta Mol. Cell. Res.*, **1843**, 1948–1968.

89. Pochopien,A.A., Beckert,B., Kasvandik,S., Berninghausen,O., Beckmann,R., Tenson,T. and Wilson,D.N. (2021) Structure of Gcn1 bound to stalled and colliding 80S ribosomes. *Proc. Natl. Acad. Sci. USA*, **118**, e2022756118.

90. Wei,Z., Zhang,P., Zhou,Z., Cheng,Z., Wan,M. and Gong,W. (2004) Crystal structure of human eIF3k, the first structure of eIF3 subunits. *J. Biol. Chem.*, **279**, 34983–34990.

91. Leppek,K., Das,R. and Barna,M. (2018) Functional 5′ UTR mRNA structures in eukaryotic translation regulation and how to find them. *Nat. Rev. Mol. Cell Biol.*, **19**, 158–174.

92. Sharma,D.K., Bressler,K., Patel,H., Balasingam,N. and Thakor,N. (2016) Role of eukaryotic initiation factors during cellular stress and cancer progression. *J. Nucleic Acids*, **2016**, 8235121.

93. Jackson,R.J., Hellen,C.U. and Pestova,T.V. (2010) The mechanism of eukaryotic translation initiation and principles of its regulation. *Nat. Rev. Mol. Cell Biol.*, **11**, 113–127.

94. Gingras,A.C., Raught,B. and Sonenberg,N. (1999) eIF4 Initiation factors: effectors of mRNA recruitment to ribosomes and regulators of translation. *Annu. Rev. Biochem.*, **68**, 913–963.

95. von der Haar,T., Gross,J.D., Wagner,G. and McCarthy,J.E.G. (2004) The mRNA cap-binding protein eIF4E in post-transcriptional gene expression. *Nat. Struct. Mol. Biol.*, **11**, 503–511.

96. Richter,J.D. and Sonenberg,N. (2005) Regulation of cap-dependent translation by eIF4E inhibitory proteins. *Nature*, **433**, 477–480.

97. Grüner,S., Weber,R., Peter,D., Chung,M.-Y., Igreja,C., Valkov,E. and Izaurralde,E. (2018) Structural motifs in eIF4G and 4E-BPs modulate their binding to eIF4E to regulate translation initiation in yeast. *Nucleic Acids Res.*, **46**, 6893–6908.

98. Papadopoulos,E., Jenni,S., Kabha,E., Takrouri,K.J., Yi,T., Salvi,N., Luna,R.E., Gavathiotis,E., Mahalingam,P., Arthanari,H. *et al.* (2014) Structure of the eukaryotic translation initiation factor eIF4E in complex with 4EGI-1 reveals an allosteric mechanism for dissociating eIF4G. *Proc. Natl. Acad. Sci. USA*, **111**, 3187–3195.

99. Villa,N. and Fraser,C. (2015) The role of RNA binding by eIF4G in mRNA recruitment to the human ribosome. *FASEB J.*, **29**, 892–916.

100. Sonenberg,N. and Hinnebusch,A.G. (2007) New modes of translational control in development, behavior, and disease. *Mol. Cell*, **28**, 721–729.

101. Villa,N., Do,A., Hershey,J.W.B. and Fraser,C.S. (2013) Human eukaryotic initiation factor 4G (eIF4G) protein binds to eIF3c, -d, and -e to promote mRNA recruitment to the ribosome. *J. Biol. Chem.*, **288**, 32932–32940.

102. LeFebvre,A.K., Korneeva,N.L., Trutschl,M., Cvek,U., Duzan,R.D., Bradley,C.A., Hershey,J.W.B. and Rhoads,R.E. (2006) Translation initiation factor eIF4G-1 binds to eIF3 through the eIF3e subunit. *J. Biol. Chem.*, **281**, 22917–22932.

103. Gradi,A., Imataka,H., Svitkin,Y.V., Rom,E., Raught,B., Morino,S. and Sonenberg,N. (1998) A novel functional human eukaryotic translation initiation factor 4G. *Mol. Cell. Biol.*, **18**, 334–342.

104. Bovee,M.L., Lamphear,B.J., Rhoads,R.E. and Lloyd,R.E. (1998) Direct cleavage of eIF4G by poliovirus 2A protease is inefficient in vitro. *Virology*, **245**, 241–249.

105. Henis-Korenblit,S., Strumpf,N.L., Goldstaub,D. and Kimchi,A. (2000) A novel form of DAP5 protein accumulates in apoptotic cells as a result of caspase cleavage and internal ribosome entry site-mediated translation. *Mol. Cell. Biol.*, **20**, 496–506.

106. Henis-Korenblit,S., Shani,G., Sines,T., Marash,L., Shohat,G. and Kimchi,A. (2002) The caspase-cleaved DAP5 protein supports internal ribosome entry site-mediated translation of death proteins. *Proc. Natl. Acad. Sci. USA*, **99**, 5400–5405.

107. Marash,L., Liberman,N., Henis-Korenblit,S., Sivan,G., Reem,E., Elroy-Stein,O. and Kimchi,A. (2008) DAP5 promotes cap-independent translation of Bcl-2 and CDK1 to facilitate cell survival during mitosis. *Mol. Cell*, **30**, 447–459.

108. Nevins,T.A., Harder,Z.M., Korneluk,R.G. and Holčík,M. (2003) Distinct regulation of internal ribosome entry Site-mediated translation following cellular stress is mediated by apoptotic fragments of eIF4G translation initiation factor family members eIF4GI and p97/DAP5/NAT1. *J. Biol. Chem.*, **278**, 3572–3579.

109. Marash,L. and Kimchi,A. (2005) DAP5 and IRES-mediated translation during programmed cell death. *Cell Death Differ.*, **12**, 554–562.

110. de la Parra,C., Ernlund,A., Alard,A., Ruggles,K., Ueberheide,B. and Schneider,R.J. (2018) A widespread alternate form of cap-dependent mRNA translation initiation. *Nat. Commun.*, **9**, 3068.

111. Paulin,F.E.M., Campbell,L.E., O'Brien,K., Loughlin,J. and Proud,C.G. (2001) Eukaryotic translation initiation factor 5 (eIF5) acts as a classical GTPase-activator protein. *Curr. Biol.*, **11**, 55–59.

112. Hinnebusch,A.G. (2014) The scanning mechanism of eukaryotic translation initiation. *Annu. Rev. Biochem.*, **83**, 779–812.

113. Luna,R.E., Arthanari,H., Hiraishi,H., Akabayov,B., Tang,L., Cox,C., Markus,M.A., Luna,L.E., Ikeda,Y., Watanabe,R. *et al.* (2013) The interaction between eukaryotic initiation factor 1A and eIF5 retains eIF1 within scanning preinitiation complexes. *Biochemistry*, **52**, 9510–9518.

114. Das,S., Ghosh,R. and Maitra,U. (2001) Eukaryotic translation initiation factor 5 functions as a GTPase-activating protein. *J. Biol. Chem.*, **276**, 6720–6726.

115. Algire,M.A., Maag,D. and Lorsch,J.R. (2005) P$_i$ Release from eIF2, not GTP hydrolysis, is the step controlled by start-site selection during eukaryotic translation initiation. *Mol. Cell*, **20**, 251–262.

116. Jennings,M.D., Kershaw,C.J., Adomavicius,T. and Pavitt,G.D. (2017) Fail-safe control of translation initiation by dissociation of eIF2α phosphorylated ternary complexes. *Elife*, **6**, e24542.

117. Huang,H., Yoon,H., Hannig,E.M. and Donahue,T.F. (1997) GTP hydrolysis controls stringent selection of the AUG start codon during translation initiation in Saccharomyces cerevisiae. *Genes Dev.*, **11**, 2396–2413.

118. Passmore,L.A., Schmeing,T.M., Maag,D., Applefield,D.J., Acker,M.G., Algire,Mikkel A., Lorsch,J.R. and Ramakrishnan,V. (2007) The eukaryotic translation initiation factors eIF1 and eIF1A induce an open conformation of the 40S ribosome. *Mol. Cell*, **26**, 41–50.

119. Sokabe,M. and Fraser,C.S. (2014) Human eukaryotic initiation factor 2 (eIF2)-GTP-Met-tRNAi ternary complex and eIF3 stabilize the 43 S preinitiation complex. *J. Biol. Chem.*, **289**, 31827–31836.

120. Asano,K., Clayton,J., Shalev,A. and Hinnebusch,A.G. (2000) A multifactor complex of eukaryotic initiation factors, eIF1, eIF2, eIF3, eIF5, and initiator tRNAMet is an important translation initiation intermediate in vivo. *Genes Dev.*, **14**, 2534–2546.

121. Pavitt,G.D. (2005) eIF2B, a mediator of general and gene-specific translational control. *Biochem. Soc. Trans.*, **33**, 1487–1492.

122. Kapp,L.D. and Lorsch,J.R. (2004) GTP-dependent recognition of the methionine moiety on initiator tRNA by translation factor eIF2. *J. Mol. Biol.*, **335**, 923–936.

123. Hinnebusch,A.G. and Lorsch,J.R. (2012) The mechanism of eukaryotic translation initiation: new insights and challenges. *Cold Spring Harb. Perspect. Biol.*, **4**, a011544.

124. Gomez,E., Mohammad,S.S. and Pavitt,G.D. (2002) Characterization of the minimal catalytic domain within eIF2B: the guanine-nucleotide exchange factor for translation initiation. *EMBO J.*, **21**, 5292–5301.

125. Kashiwagi,K., Takahashi,M., Nishimoto,M., Hiyama,T.B., Higo,T., Umehara,T., Sakamoto,K., Ito,T. and Yokoyama,S. (2016) Crystal structure of eukaryotic translation initiation factor 2B. *Nature*, **531**, 122–125.

126. Schütz,P., Bumann,M., Oberholzer,A.E., Bieniossek,C., Trachsel,H., Altmann,M. and Baumann,U. (2008) Crystal structure of the yeast eIF4A-eIF4G complex: an RNA-helicase controlled by protein–protein interactions. *Proc. Natl. Acad, Sci. USA*, **105**, 9564–9569.

127. Virgili,G., Frank,F., Feoktistova,K., Sawicki,M., Sonenberg,N., Fraser,C.S. and Nagar,B. (2013) Structural analysis of the DAP5 MIF4G domain and its interaction with eIF4A. *Structure*, **21**, 517–527.

128. Liberman,N., Gandin,V., Svitkin,Y.V., David,M., Virgili,G., Jaramillo,M., Holcik,M., Nagar,B., Kimchi,A. and Sonenberg,N. (2015) DAP5 associates with eIF2β and eIF4AI to promote internal ribosome entry site driven translation. *Nucleic Acids Res.*, **43**, 3764–3775.

129. Dobrikov,M.I., Dobrikova,E.Y. and Gromeier,M. (2013) Dynamic regulation of the translation initiation helicase complex by mitogenic signal transduction to eukaryotic translation initiation factor 4G. *Mol. Cell. Biol.*, **33**, 937–946.

130. Korneeva,N.L., Lamphear,B.J., Hennigan,F.L.C. and Rhoads,R.E. (2000) Mutually cooperative binding of eukaryotic translation initiation factor (eIF) 3 and eIF4A to human eIF4G-1. *J. Biol. Chem.*, **275**, 41369–41376.

131. Dobrikov,M.I., Dobrikova,E.Y. and Gromeier,M. (2018) Ribosomal RACK1:Protein kinase c βII modulates intramolecular interactions between unstructured regions of eukaryotic initiation factor 4G (eIF4G) that control eIF4E and eIF3 binding. *Mol. Cell. Biol.*, **38**, e00306-18.

132. Weingarten-Gabbay,S., Khan,D., Liberman,N., Yoffe,Y., Bialik,S., Das,S., Oren,M. and Kimchi,A. (2014) The translation initiation factor DAP5 promotes IRES-driven translation of p53 mRNA. *Oncogene*, **33**, 611–618.

133. Lee,S.H. and McCormick,F. (2006) p97/DAP5 is a ribosome-associated factor that facilitates protein synthesis and cell proliferation by modulating the synthesis of cell cycle proteins. *EMBO J.*, **25**, 4008–4019.

134. Pyronnet,S., Imataka,H., Gingras,A.-C., Fukunaga,R., Hunter,T. and Sonenberg,N. (1999) Human eukaryotic translation initiation factor 4G (eIF4G) recruits Mnk1 to phosphorylate eIF4E. *EMBO J.*, **18**, 270–279.

135. Waskiewicz,A.J., Johnson,J.C., Penn,B., Mahalingam,M., Kimball,S.R. and Cooper,J.A. (1999) Phosphorylation of the cap-binding protein eukaryotic translation initiation factor 4E by protein kinase Mnk1 in vivo. *Mol. Cell. Biol.*, **19**, 1871–1880.

136. Marcotrigiano,J., Gingras,A.-C., Sonenberg,N. and Burley,S.K. (1997) Cocrystal structure of the messenger RNA 5′ cap-binding protein (eIF4E) bound to 7-methyl-GDP. *Cell*, **89**, 951–961.

137. Shveygert,M., Kaiser,C., Bradrick,S.S. and Gromeier,M. (2010) Regulation of eukaryotic initiation factor 4E (eIF4E) phosphorylation by mitogen-activated protein kinase occurs through modulation of Mnk1-eIF4G interaction. *Mol. Cell. Biol.*, **30**, 5160–5167.

138. Alone,P.V. and Dever,T.E. (2006) Direct binding of translation initiation factor eIF2γ-G domain to its GTPase-activating and GDP-GTP exchange factors eIF5 and eIF2Bε. *J. Biol. Chem.*, **281**, 12636–12644.

139. Kashiwagi,K., Yokoyama,T., Nishimoto,M., Takahashi,M., Sakamoto,A., Yonemochi,M., Shirouzu,M. and Ito,T. (2019) Structural basis for eIF2B inhibition in integrated stress response. *Science*, **364**, 495–499.

140. Kenner,L.R., Anand,A.A., Nguyen,H.C., Myasnikov,A.G., Klose,C.J., McGeever,L.A., Tsai,J.C., Miller-Vedam,L.E., Walter,P. and Frost,A. (2019) eIF2B-catalyzed nucleotide exchange and phosphoregulation by the integrated stress response. *Science*, **364**, 491–495.

141. Luna,RafaelE., Arthanari,H., Hiraishi,H., Nanda,J., Martin-Marcos,P., Markus,MichelleA., Akabayov,B., Milbradt,AlexanderG., Luna,LunetE., Seo,H.-C. *et al.* (2012) The C-Terminal domain of eukaryotic initiation factor 5 promotes start codon recognition by its dynamic interplay with eIF1 and eIF2β. *Cell Rep.*, **1**, 689–702.

142. Valášek,L., Nielsen,K.H., Zhang,F., Fekete,C.A. and Hinnebusch,A.G. (2004) Interactions of eukaryotic translation initiation factor 3 (eIF3) subunit NIP1/c with eIF1 and eIF5 promote preinitiation complex assembly and regulate start codon selection. *Mol. Cell. Biol.*, **24**, 9437–9455.

143. Valášek,L.S., Zeman,J., Wagner,S., Beznosková,P., Pavlíková,Z., Mohammad,M.P., Hronová,V., Herrmannová,A., Hashem,Y. and Gunišová,S. (2017) Embraced by eIF3: structural and functional insights into the roles of eIF3 across the translation cycle. *Nucleic Acids Res.*, **45**, 10948–10968.

144. Zeman,J., Itoh,Y., Kukačka,Z., Rosůlek,M., Kavan,D., Kouba,T., Jansen,M.E., Mohammad,M.P., Novák,P. and Valášek,L.S. (2019) Binding of eIF3 in complex with eIF5 and eIF1 to the 40S ribosomal subunit is accompanied by dramatic structural changes. *Nucleic Acids Res.*, **47**, 8282–8300.

145. des Georges,A., Dhote,V., Kuhn,L., Hellen,C.U.T., Pestova,T.V., Frank,J. and Hashem,Y. (2015) Structure of mammalian eIF3 in the context of the 43S preinitiation complex. *Nature*, **525**, 491–495.

146. Aylett,C.H.S., Boehringer,D., Erzberger,J.P., Schaefer,T. and Ban,N. (2015) Structure of a Yeast 40S–eIF1–eIF1A–eIF3–eIF3j initiation complex. *Nat. Struct. Mol. Biol.*, **22**, 269–271.

147. Jennings,M.D. and Pavitt,G.D. (2010) eIF5 has GDI activity necessary for translational control by eIF2 phosphorylation. *Nature*, **465**, 378–381.

148. Jennings,M.D., Kershaw,C.J., White,C., Hoyle,D., Richardson,J.P., Costello,J.L., Donaldson,I.J., Zhou,Y. and Pavitt,G.D. (2016) eIF2β is critical for eIF5-mediated GDP-dissociation inhibitor activity and translational control. *Nucleic Acids Res.*, **44**, 9698–9709.

149. Gordiyenko,Y., Schmidt,C., Jennings,M.D., Matak-Vinkovic,D., Pavitt,G.D. and Robinson,C.V. (2014) eIF2B is a decameric guanine nucleotide exchange factor with a γ2ε2 tetrameric core. *Nature Commun.*, **5**, 3902.

150. Kuhle,B., Eulig,N.K. and Ficner,R. (2015) Architecture of the eIF2B regulatory subcomplex and its implications for the regulation of guanine nucleotide exchange on eIF2. *Nucleic Acids Res.*, **43**, 9994–10014.

151. Jennings,M.D., Zhou,Y., Mohammad-Qureshi,S.S., Bennett,D. and Pavitt,G.D. (2013) eIF2B promotes eIF5 dissociation from eIF2•GDP to facilitate guanine nucleotide exchange for translation initiation. *Genes Dev.*, **27**, 2696–2707.

152. Singh,C.R., Lee,B., Udagawa,T., Mohammad-Qureshi,S.S., Yamamoto,Y., Pavitt,G.D. and Asano,K. (2006) An eIF5/eIF2 complex antagonizes guanine nucleotide exchange by eIF2B during translation initiation. *EMBO J.*, **25**, 4537–4546.

153. Fan,S., Jia,M.-Z. and Gong,W. (2010) Crystal structure of the C-terminal region of human p97/DAP5. *Proteins*, **78**, 2385–2390.

154. Wei,J., Jia,M., Zhang,C., Wang,M., Gao,F., Xu,H. and Gong,W. (2010) Crystal structure of the C-terminal domain of the ε subunit of human translation initiation factor eIF2B. *Proteins*, **1**, 595–603.

155. Bryant,J.D., Brown,M.C., Dobrikov,M.I., Dobrikova,E.Y., Gemberling,S.L., Zhang,Q. and Gromeier,M. (2018) Regulation of hypoxia-inducible factor 1α during hypoxia by DAP5-Induced translation of PHD2. *Mol. Cell. Biol.*, **38**, e00647-17.

156. Pelletier,J. and Sonenberg,N. (2019) The organizing principles of eukaryotic ribosome recruitment. *Annu. Rev. Biochem.*, **88**, 307–335.

157. Brito Querido,J., Sokabe,M., Kraatz,S., Gordiyenko,Y., Skehel,J.M., Fraser,C.S. and Ramakrishnan,V. (2020) Structure of a human 48S translational initiation complex. *Science*, **369**, 1220–1227.

158. Iwasaki,S., Iwasaki,W., Takahashi,M., Sakamoto,A., Watanabe,C., Shichino,Y., Floor,S.N., Fujiwara,K., Mito,M., Dodo,K. *et al.* (2019) The translation inhibitor rocaglamide targets a bimolecular cavity between eIF4A and polypurine RNA. *Mol. Cell*, **73**, 738–748.

159. de Breyne,S. and Ohlmann,T. (2018) Focus on translation initiation of the HIV-1 mRNAs. *Int. J. Mol. Sci.*, **20**, 101.

160. Lyons,S.M., Kharel,P., Akiyama,Y., Ojha,S., Dave,D., Tsvetkov,V., Merrick,W., Ivanov,P. and Anderson,P. (2020) eIF4G has intrinsic G-quadruplex binding activity that is required for tiRNA function. *Nucleic Acids Res.*, **48**, 6223–6233.

161. Copeland,K.L., Pellock,S.J., Cox,J.R., Cafiero,M.L. and Tschumper,G.S. (2013) Examination of tyrosine/adenine stacking interactions in protein complexes. *J. Phys. Chem. B*, **117**, 14001–14008.

162. Boehr,D.D., Farley,A.R., Wright,G.D. and Cox,J.R. (2002) Analysis of the π-π stacking interactions between the aminoglycoside antibiotic kinase APH(3′)-IIIa and its nucleotide ligands. *Chem. Biol.*, **9**, 1209–1217.

163. Çetin,B. and O'Leary,S.E. (2021) mRNA- and factor-driven dynamic variability controls eIF4F-cap recognition for translation initiation. bioRxiv doi: https://doi.org/10.1101/2021.06.17.448745, 17 June 2021, preprint: not peer reviewed.

164. Costello,J., Castelli,L.M., Rowe,W., Kershaw,C.J., Talavera,D., Mohammad-Qureshi,S.S., Sims,P.F.G., Grant,C.M., Pavitt,G.D., Hubbard,S.J. *et al.* (2015) Global mRNA selection mechanisms for translation initiation. *Genome Biol.*, **16**, 10.

165. Thompson,M.K. and Gilbert,W.V. (2017) mRNA length-sensing in eukaryotic translation: reconsidering the "closed loop" and its implications for translational control. *Curr. Genet.*, **63**, 613–620.

166. Pestova,T.V., Shatsky,I.N. and Hellen,C.U. (1996) Functional dissection of eukaryotic initiation factor 4F: the 4A subunit and the central domain of the 4G subunit are sufficient to mediate internal entry of 43S preinitiation complexes. *Mol. Cell. Biol.*, **16**, 6870–6878.

167. Pestova,T.V., Hellen,C.U. and Shatsky,I.N. (1996) Canonical eukaryotic initiation factors determine initiation of translation by internal ribosomal entry. *Mol. Cell. Biol.*, **16**, 6859–6869.

168. Lomakin,I.B., Hellen,C.U. and Pestova,T.V. (2000) Physical association of eukaryotic initiation factor 4G (eIF4G) with eIF4A strongly enhances binding of eIF4G to the internal ribosomal entry site of encephalomyocarditis virus and is required for internal initiation of translation. *Mol. Cell. Biol.*, **20**, 6019–6029.

169. Bassili,G., Tzima,E., Song,Y., Saleh,L., Ochs,K. and Niepmann,M. (2004) Sequence and secondary structure requirements in a highly conserved element for foot-and-mouth disease virus internal ribosome entry site activity and eIF4G binding. *J. Gen. Virol.*, **85**, 2555–2565.

170. Kolupaeva,V.G., Pestova,T.V., Hellen,C.U.T. and Shatsky,I.N. (1998) Translation eukaryotic initiation factor 4G recognizes a specific structural element within the internal ribosome entry site of encephalomyocarditis virus RNA. *J. Biol. Chem.*, **273**, 18599–18604.

171. López de Quinto,S. and Martínez-Salas,E. (2000) Interaction of the eIF4G initiation factor with the aphthovirus IRES is essential for internal translation initiation in vivo. *RNA*, **6**, 1380–1392.

172. Marintchev,A., Frueh,D. and Wagner,G. (2007) NMR methods for studying protein-protein interactions involved in translation initiation, *Meth. Enzym.*, **430**, 283–331.

173. Pöyry,T.A.A., Kaminski,A., Connell,E.J., Fraser,C.S. and Jackson,R.J. (2007) The mechanism of an exceptional case of reinitiation after translation of a long ORF reveals why such events do not generally occur in mammalian mRNA translation. *Genes Dev.*, **21**, 3149–3162.

174. Breyne,S.d., Yu,Y., Unbehaun,A., Pestova,T.V. and Hellen,C.U.T. (2009) Direct functional interaction of initiation factor eIF4G with type 1 internal ribosomal entry sites. *Proc. Natl. Acad. Sci. USA*, **106**, 9197–9202.

175. Kolupaeva,V.G., Lomakin,I.B., Pestova,T.V. and Hellen,C.U.T. (2003) Eukaryotic initiation factors 4G and 4A mediate conformational changes downstream of the initiation codon of the encephalomyocarditis virus internal ribosomal entry site. *Mol. Cell. Biol.*, **23**, 687–698.

176. Robert,F., Cencic,R., Cai,R., Schmeing,T.M. and Pelletier,J. (2020) RNA-tethering assay and eIF4G:eIF4A obligate dimer design uncovers multiple eIF4F functional complexes. *Nucleic Acids Res.*, **48**, 8562–8575.

177. Andreou,A.Z. and Klostermeier,D. (2013) The DEAD-box helicase eIF4A: paradigm or the odd one out? *RNA Biol.*, **10**, 19–32.

178. Tauber,D., Tauber,G., Khong,A., Van Treeck,B., Pelletier,J. and Parker,R. (2020) Modulation of RNA condensation by the DEAD-Box protein eIF4A. *Cell*, **180**, 411–426.

179. Kyte,J. and Doolittle,R.F. (1982) A simple method for displaying the hydropathic character of a protein. *J. Mol. Biol.*, **157**, 105–132.

180. Glaser,F., Pupko,T., Paz,I., Bell,R.E., Bechor-Shental,D., Martz,E. and Ben-Tal,N. (2003) ConSurf: identification of functional regions in proteins by surface-mapping of phylogenetic information. *Bioinformatics*, **19**, 163–164.

181. Ashkenazy,H., Abadi,S., Martz,E., Chay,O., Mayrose,I., Pupko,T. and Ben-Tal,N. (2016) ConSurf 2016: an improved methodology to estimate and visualize evolutionary conservation in macromolecules. *Nucleic Acids Res.*, **44**, W344–W350.

182. Re,A., Joshi,T., Kulberkyte,E., Morris,Q. and Workman,C.T. (2014) RNA-protein interactions: an overview. *Methods Mol. Biol.*, **1097**, 491–521.

183. Jones,S. (2016) Protein–RNA interactions: structural biology and computational modeling techniques. *Biophys. Rev.*, **8**, 359–367.

184. Jones,S., Daley,D.T., Luscombe,N.M., Berman,H.M. and Thornton,J.M. (2001) Protein-RNA interactions: a structural analysis. *Nucleic Acids Res.*, **29**, 943–954.

185. Jones,S. and Thornton,J.M. (1996) Principles of protein-protein interactions. *Proc. Natl. Acad. Sci. USA*, **93**, 13–20.

186. Krüger,D.M., Neubacher,S. and Grossmann,T.N. (2018) Protein–RNA interactions: structural characteristics and hotspot amino acids. *RNA*, **24**, 1457–1465.

187. Dobrikov,M., Dobrikova,E., Shveygert,M. and Gromeier,M. (2011) Phosphorylation of eukaryotic translation initiation factor 4G1 (eIF4G1) by protein kinase Cα regulates eIF4G1 binding to Mnk1. *Mol. Cell. Biol.*, **31**, 2947–2959.

188. Parra-Palau,J.-L., Scheper,G.C., Wilson,M.L. and Proud,C.G. (2003) Features in the N and C termini of the MAPK-interacting kinase mnk1 mediate its nucleocytoplasmic shuttling. *J. Biol. Chem.*, **278**, 44197–44204.

189. Kuhle,B. (2014) Structural and functional studies on GTPases involved in eukaryal translation initiation. Dissertation, Georg-August-Universität Göttingen.

190. Das,S., Maiti,T., Das,K. and Maitra,U. (1997) Specific interaction of eukaryotic translation initiation factor 5 (eIF5) with the β-Subunit of eIF2. *J. Biol. Chem.*, **272**, 31712–31718.

191. Paul,E.E., Lin,K.Y., Gamble,N., Tsai,A.W., Swan,S.H.K., Yang,Y., Doran,M. and Marintchev,A. (2022) Dynamic interaction network involving the conserved intrinsically disordered regions in human eIF5. *Biophys. Chem.*, **281**, 106740.

192. Homma,M.K., Wada,I., Suzuki,T., Yamaki,J., Krebs,E.G. and Homma,Y. (2005) CK2 phosphorylation of eukaryotic translation initiation factor 5 potentiates cell cycle progression. *Proc. Natl. Acad. Sci. USA*, **102**, 15688–15693.

193. Davey,N.E. (2019) The functional importance of structure in unstructured protein regions. *Curr. Opin. Struct. Biol.*, **56**, 155–163.

194. Wright,P.E. and Dyson,H.J. (2015) Intrinsically disordered proteins in cellular signaling and regulation. *Nat. Rev. Mol. Cell Biol.*, **16**, 18–29.

195. Phillips,A.H. and Kriwacki,R.W. (2019) Intrinsic protein disorder and protein modifications in the processing of biological signals. *Curr. Opin. Struct. Biol.*, **60**, 1–6.

196. Dyson,H.J. and Wright,P.E. (2019) Perspective: the essential role of NMR in the discovery and characterization of intrinsically disordered proteins. *J. Biomol. NMR*, **73**, 651–659.

197. Borgia,A., Borgia,M.B., Bugge,K., Kissling,V.M., Heidarsson,P.O., Fernandes,C.B., Sottini,A., Soranno,A., Buholzer,K.J., Nettels,D. *et al.* (2018) Extreme disorder in an ultrahigh-affinity protein complex. *Nature*, **555**, 61–66.

198. Na,J.-H., Lee,W.-K. and Yu,Y.G. (2018) How do we study the dynamic structure of unstructured proteins: a case study on nopp140 as an example of a large, intrinsically disordered protein. *Int. J. Mol. Sci.*, **19**, 381.

199. Oldfield,C.J. and Dunker,A.K. (2014) Intrinsically disordered proteins and intrinsically disordered protein regions. *Annu. Rev. Biochem.*, **83**, 553–584.

200. Senior,A.W., Evans,R., Jumper,J., Kirkpatrick,J., Sifre,L., Green,T., Qin,C., Žídek,A., Nelson,A.W.R., Bridgland,A. *et al.* (2020) Improved protein structure prediction using potentials from deep learning. *Nature*, **577**, 706–710.

201. Senior,A.W., Evans,R., Jumper,J., Kirkpatrick,J., Sifre,L., Green,T., Qin,C., Žídek,A., Nelson,A.W.R., Bridgland,A. *et al.* (2019) Protein structure prediction using multiple deep neural networks in the 13th critical assessment of protein structure prediction (CASP13). *Proteins*, **87**, 1141–1148.

202. Tsang,B., Arsenault,J., Vernon,R.M., Lin,H., Sonenberg,N., Wang,L.-Y., Bah,A. and Forman-Kay,J.D. (2019) Phosphoregulated FMRP phase separation models activity-dependent translation through bidirectional control of mRNA granule formation. *Proc. Natl. Acad. Sci. USA*, **116**, 4218–4227.

203. Das,S., Lin,Y.-H., Vernon,R.M., Forman-Kay,J.D. and Chan,H.S. (2020) Comparative roles of charge, π, and hydrophobic interactions in sequence-dependent phase separation of intrinsically disordered proteins. *Proc. Natl. Acad. Sci. USA*, **117**, 28795–28805.

204. Bah,A., Vernon,R.M., Siddiqui,Z., Krzeminski,M., Muhandiram,R., Zhao,C., Sonenberg,N., Kay,L.E. and Forman-Kay,J.D. (2015) Folding of an intrinsically disordered protein by phosphorylation as a regulatory switch. *Nature*, **519**, 106–109.

205. Liu,N., Guo,Y., Ning,S. and Duan,M. (2020) Phosphorylation regulates the binding of intrinsically disordered proteins via a flexible conformation selection mechanism. *Commun. Chem.*, **3**, 123.

206. Kulkarni,P., Jolly,M.K., Jia,D., Mooney,S.M., Bhargava,A., Kagohara,L.T., Chen,Y., Hao,P., He,Y., Veltri,R.W. *et al.* (2017) Phosphorylation-induced conformational dynamics in an intrinsically disordered protein and potential role in phenotypic heterogeneity. *Proc. Natl. Acad. Sci. USA*, **114**, 2644–2653.

207. Olsen,J.V., Vermeulen,M., Santamaria,A., Kumar,C., Miller,M.L., Jensen,L.J., Gnad,F., Cox,J., Jensen,T.S., Nigg,E.A. *et al.* (2010) Quantitative phosphoproteomics reveals widespread full phosphorylation site occupancy during mitosis. *Sci. Signal.*, **3**, ra3.

208. Zhou,H., Di Palma,S., Preisinger,C., Peng,M., Polat,A.N., Heck,A.J.R. and Mohammed,S. (2013) Toward a comprehensive characterization of a human cancer cell phosphoproteome. *J. Proteome Res.*, **12**, 260–271.

209. Dephoure,N., Zhou,C., Villén,J., Beausoleil,S.A., Bakalarski,C.E., Elledge,S.J. and Gygi,S.P. (2008) A quantitative atlas of mitotic phosphorylation. *Proc. Natl. Acad. Sci. USA*, **105**, 10762–10767.